NAVAL POSTGRADUATE SCHOOL

MONTEREY, CALIFORNIA

THESIS

SENSOR SYNCHRONIZATION, GEOLOCATION AND WIRELESS COMMUNICATION IN A SHIPBOARD OPPORTUNISTIC ARRAY

by

Yong Loke
March 2006

Thesis Advisor:	David Jenn
Second Reader:	Michael Morgan

Approved for public release, distribution is unlimited

THIS PAGE INTENTIONALLY LEFT BLANK

REPORT DOCUMENTATION PAGE			Form Approved OMB No. 0704-0188
Public reporting burden for this collection of information is estimated to average 1 hour per response, including the time for reviewing instruction, searching existing data sources, gathering and maintaining the data needed, and completing and reviewing the collection of information. Send comments regarding this burden estimate or any other aspect of this collection of information, including suggestions for reducing this burden, to Washington headquarters Services, Directorate for Information Operations and Reports, 1215 Jefferson Davis Highway, Suite 1204, Arlington, VA 22202-4302, and to the Office of Management and Budget, Paperwork Reduction Project (0704-0188) Washington DC 20503.			
1. AGENCY USE ONLY ***(Leave blank)***	**2. REPORT DATE** March 2006	**3. REPORT TYPE AND DATES COVERED** Master's Thesis	
4. TITLE AND SUBTITLE: Sensor Synchronization, Geolocation and Wireless Communication in a Shipboard Opportunistic Array			**5. FUNDING NUMBERS**
6. AUTHOR(S) Yong Loke			
7. PERFORMING ORGANIZATION NAME(S) AND ADDRESS(ES) Naval Postgraduate School Monterey, CA 93943-5000			**8. PERFORMING ORGANIZATION REPORT NUMBER**
9. SPONSORING /MONITORING AGENCY NAME(S) AND ADDRESS(ES) N/A			**10. SPONSORING/MONITORING AGENCY REPORT NUMBER**
11. SUPPLEMENTARY NOTES The views expressed in this thesis are those of the author and do not reflect the official policy or position of the Department of Defense or the U.S. Government.			
12a. DISTRIBUTION / AVAILABILITY STATEMENT Approved for public release; distribution is unlimited			**12b. DISTRIBUTION CODE**

13. ABSTRACT (maximum 200 words)

A wirelessly networked opportunistic digital array radar (WNODAR) is an integrated ship wide digital phased array, where the array elements are placed at available open areas over the entire surface of the platform. The array elements are self-standing digital transmit/receive (T/R) modules with no hardwire connections other than prime power. All control and digitized signals are passed wirelessly between the elements and a central signal processor.

This research investigates the problem of integrating the array elements through the design of a wireless synchronization and geolocation network. Phase synchronization of array elements is possible using a simple synchronization circuit. A technical survey of geolocation techniques was performed, and performance curves for the WNODAR operating under different seastate conditions were obtained. Analysis and simulation results suggest that a position location scheme to correct for dynamic effects of hull deflection is not absolutely necessary for an array operating at a VHF or lower UHF frequency. Finally, a design of the demonstration T/R module is proposed. Based on projected communication requirements, the full-scale WNODAR demands a 3.7 Gb/s data transmission rate. The multi-input multi-output orthogonal frequency division multiplexing (MIMO-OFDM) approach has been identified as a promising solution to achieve gigabit transmission rates.

14. SUBJECT TERMS Phased Array, Opportunistic Phased Array, Aperstructure, Radar, Transmitter, Receiver, Phase Synchronization, Sensor Geolocation, Wireless Communication, COTS			**15. NUMBER OF PAGES** 100
			16. PRICE CODE
17. SECURITY CLASSIFICATION OF REPORT Unclassified	**18. SECURITY CLASSIFICATION OF THIS PAGE** Unclassified	**19. SECURITY CLASSIFICATION OF ABSTRACT** Unclassified	**20. LIMITATION OF ABSTRACT** UL

NSN 7540-01-280-5500 Standard Form 298 (Rev. 2-89)
Prescribed by ANSI Std. 239-18

THIS PAGE INTENTIONALLY LEFT BLANK

Approved for public release, distribution is unlimited

SENSOR SYNCHRONIZATION, GEOLOCATION AND WIRELESS COMMUNICATION IN A SHIPBOARD OPPORTUNISTIC ARRAY

Yong Loke
Major, Republic of Singapore Navy
M.Eng., Imperial College of Science, Technology and Medicine,
University of London, 1997

Submitted in partial fulfillment of the
requirements for the degree of

MASTER OF SCIENCE IN ELECTRICAL ENGINEERING

from the

NAVAL POSTGRADUATE SCHOOL
March 2006

Author: Yong Loke

Approved by: David Jenn
Thesis Advisor

Michael Morgan
Second Reader

Jeffrey B. Knorr
Chairman, Department of Electrical and Computer Engineering

THIS PAGE INTENTIONALLY LEFT BLANK

ABSTRACT

A wirelessly networked opportunistic digital array radar (WNODAR) is an integrated ship wide digital phased array, where the array elements are placed at available open areas over the entire surface of the platform. The array elements are self-standing digital transmit/receive (T/R) modules with no hardwire connections other than prime power. All control and digitized signals are passed wirelessly between the elements and a central signal processor.

This research investigates the problem of integrating the array elements through the design of a wireless synchronization and geolocation network. Phase synchronization of array elements is possible using a simple synchronization circuit. A technical survey of geolocation techniques was performed, and performance curves for the WNODAR operating under different seastate conditions were obtained. Analysis and simulation results suggest that a position location scheme to correct for dynamic effects of hull deflection is not absolutely necessary for an array operating at a VHF or lower UHF frequency. Finally, a design of the demonstration T/R module is proposed. Based on projected communication requirements, the full-scale WNODAR demands a 3.7 Gb/s data transmission rate. The multi-input multi-output orthogonal frequency division multiplexing (MIMO-OFDM) approach has been identified as a promising solution to achieve gigabit transmission rates.

THIS PAGE INTENTIONALLY LEFT BLANK

TABLE OF CONTENTS

LIST OF FIGURES

LIST OF TABLES

THIS PAGE INTENTIONALLY LEFT BLANK

ACKNOWLEDGMENTS

This work would not have been possible without my supervisor Professor David Jenn of the Naval Postgraduate School, Monterey, California. I have to thank Professor Jenn for being a patient supervisor and for providing the ideas behind this work. I would like to thank James King of the ONR for supporting and sponsoring this research.

I would also like to thank Professor Morgan for agreeing to second-read the thesis, Professor Solitario for providing the source for the ship hull deflection data, and CDR Broadston for helping with the equipment in the Microwave laboratory.

I cannot end without thanking my wife Wen Shan, on whose constant encouragement and love I have relied throughout my time at the NPS.

THIS PAGE INTENTIONALLY LEFT BLANK

EXECUTIVE SUMMARY

The "opportunistic array" concept has been the focus of research and development undertaken by the Naval Postgraduate School (NPS). An opportunistic array is an integrated ship wide digital phased array, where the array elements are placed at available open areas over the entire surface of the platform. The elements of the opportunistic array are self-standing digital transmit/receive (T/R) modules with no hardwire connections other than prime power. Element localization and synchronization signals, beam control data, and digitized target return signals are passed wirelessly between the elements and a central signal processor. Hence this approach is more concisely termed as a wirelessly networked opportunistic digital array radar (WNODAR).

One of the key applications for the WNODAR is in ballistic missile defense (BMD). Forward positioned Navy ships equipped with the WNODAR can detect and track theatre ballistic missiles from thousands of miles away. The WNODAR has many advantages over conventional phased array radars. Firstly, being a digital phased array, it is capable of multiple simultaneous receive beams, rapid dynamic reconfigurability of output beams and very low sidelobes. Secondly, the digital architecture eliminates the need for analog beamforming components and their associated calibration and drift issues. Thirdly, the conformal, dispersed element opportunistic array concept using hull appliqués retains the stealth characteristics of the warship and allows the possibility of economic retrofits.

A key challenge in the development of the WNODAR is the need to perform synchronization of the hundreds or even thousands of array elements to provide time and frequency references. Synchronization is required to scan the beam and perform coherent detection and integration. Control of the elements' phase is possible via a wireless local oscillator (LO) signal, but in dynamic conditions the transmission paths will be changing and unpredictable. In addition, there is a need to perform dynamic measurement of element locations to correct for errors due to ship hull deflection. Element location data is required for digital beamforming to avoid degradation in the sidelobes, gain, and beam pointing. This thesis attempts to address the above concerns.

The objective of this thesis was to investigate the problem of integrating the array elements through the design of a wireless synchronization and geolocation network. The sub-objectives were to:

- Examine possible approaches to dynamically synchronize array elements,
- Analyse the effect of phase shifter quantization on synchronization,
- Perform a technical survey of geolocation techniques for array elements,
- Analyse the effect of ship hull deflections on radar performance,
- Propose the design of a demonstration T/R module,
- Project the wireless communication requirements for the WNODAR and survey possible solutions to enable gigabit data transmission rates.

Two techniques to perform element synchronization for the WNODAR were proposed. The "brute force" synchronization technique is a simple method that can be easily implemented with a synchronization circuit in each element and in the central beamformer and controller. The "beam tagging" synchronization technique takes less time, but requires more hardware modifications. Since the synchronization time is on the order of 2 to 3 μs, the more simple "brute force" technique is sufficient. The problem faced by the "brute force" synchronization technique due to varying signal amplitudes can be overcome in the ship application because the distances to the elements are known and will not change enough to significantly affect amplitude. In addition, the low noise amplifier (LNA) gain in each module can be adjusted to compensate for differences in path length.

It was concluded that a four-bit synchronization phase shifter does not degrade the performance of the radar. The phase error is expected to introduce a gain reduction of 0.06 dB. For a 10 m^2 target, the theoretical maximum detection range of 2000 km is reduced to 1988 km at an average power of 500 W. Alternatively, a 2.8% increase in average power will achieve the same detection range of 2000 km. The expected RMS pointing error of less than $0.001°$ and a mean sidelobe increase of $0.1\,dB$ with respect to the main lobe is insignificant compared to the error free pattern.

The problem of position determination for elements in a WNODAR can be tackled through commercial solutions for geolocation. Under relatively benign propagation conditions, most systems are producing centimeter level accuracy, which is a fraction of the array's operating wavelength of about 1 m and within the tolerable limit of 0.1λ position error. For elements placed in a high multipath environment like the ship's open deck, ultra wideband (UWB) systems appear to be the technology of choice because of its ability to perform in the presence of objects obstructing LOS, as well as its simplicity and flexibility in design.

A radar system simulation was conducted using a CAD model of a DD(X) with 1200 randomly distributed elements, performing a broadside scan at an elevation of $10°$. Using four bit digitization and assuming 10 cm dynamic position error, a gain reduction of -0.63 dB and an increased average sidelobe level of -29.0 dB is expected. The gain reduction reduces the theoretical maximum detection range from 2000 km to 1863 km. Alternatively, a 33% increase in average power will achieve the same detection range of 2000 km. The gain reduction is the more significant degradation compared to increase in average sidelobe level.

Using conventional hull deflection data and extrapolating to the DD(X), a set of performance curves for the WNODAR was obtained as shown in Figure 1. The performance curves show data for the WNODAR operating under dynamic conditions, taking into account the effects of hull deflection under different seastate conditions, and the use of four-bit synchronization phase shifters. For an average transmission power of 500 W, a maximum detection range of 1990 km for a 10 m^2 target is obtained under seastate 6 conditions. This is only a reduction of 0.5% from the error free condition. The reason why the gain reduction is little, even for position errors greater than 20 cm, is that hull deflection contributes mainly to element height position errors. For a broadside scan at an elevation of $10°$, the contribution to phase error is low because of the cosine factor. The assumption is valid because, for BMD applications, long range targets will be expected near the horizon. Hence at this time, analysis and simulation results suggest that a position location scheme to correct for dynamic effects of hull deflection is not absolutely necessary for an array operating at a VHF or lower UHF frequency.

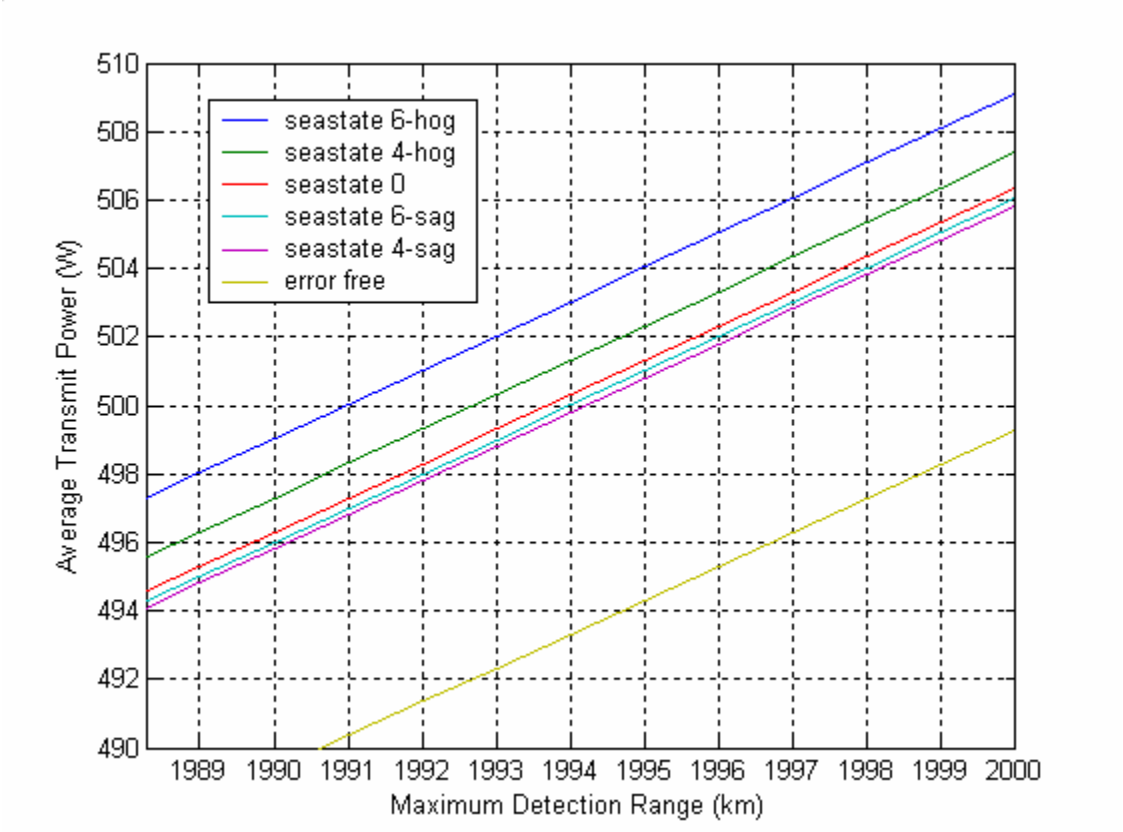

Figure 1. Performance curves for the WNODAR under different seastate conditions.

The design of the demonstration T/R module, shown in Figure 2, is proposed to validate the wireless opportunistic array concept. The design leverages on advance technology adopted from commercial markets, namely the use of field programmable gate array (FPGA) and high data rate wireless communication systems. The digital transmitter and receiver is implemented on FPGA hardware. It consists of a controller interfaced with A/D and D/A data acquisition modules. The AD83246 EVAL modulator board upconverts the transmit waveform generated by the FPGA to the operating band. On receive, the waveform is downconverted to baseband by the complimentary AD8347EVAL demodulator board, and the baseband in-phase and quadrature signals are sent to the FPGA for further processing. The wireless modem comprising RF modules and integrated circuits provide media access control over the wireless data link. In order to avoid the need for additional hardware (i.e., the synchronization circuit) and to exploit the additional computation capability of the FPGA hardware, another possibility is to

generate the LO signal from the FPGA and perform phase corrections directly using the FPGA. This can be done by sending a trigger signal to the controller and using it to generate the LO. But this will require two circulators, one for the LO, and the second for beamforming. The feasibility of this technique will have to be further explored.

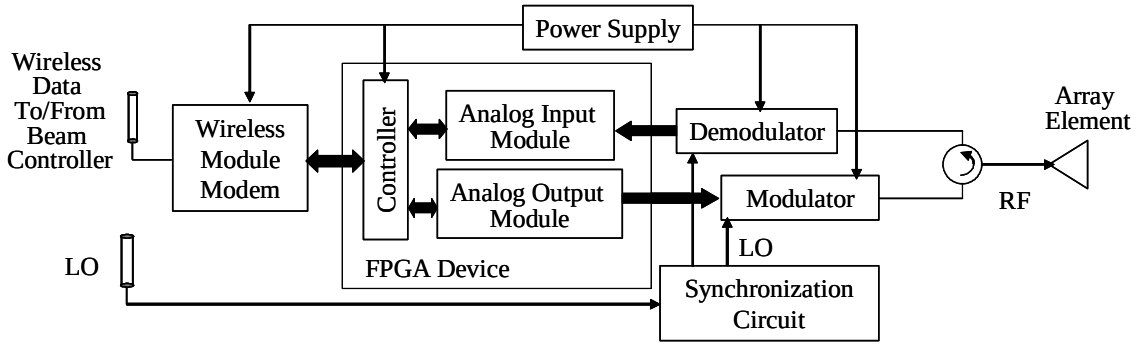

Figure 2. Block diagram of the propose demonstration T/R module.

Based on projected communication requirements, the full-scale WNODAR demands a 3.7 Gb/s data transmission rate. Currently, most commercial systems are not yet capable of gigabit transmission rates. But research suggests that multi-input multi-output orthogonal frequency division multiplexing (MIMO-OFDM) technology is a promising solution that could dramatically improve spectral efficiency and thus the viability of gigabit transmission rate. Given the current high level of research focus and the unfolding of promising developments towards cheaper, higher performance devices, it is estimated that the requirements of the WNODAR can probably be met with commercial wireless communication systems within the next five years.

The objectives of this research were met. Key components of the wireless synchronization and geolocation network that integrates the array elements of the WNODAR were investigated. Phase synchronization of array elements is possible using a simple synchronization circuit. A technical survey of geolocation techniques was performed, and performance curves for the WNODAR operating under different seastate conditions were obtained. Analysis and simulation results suggest that a position location scheme to correct for dynamic effects of hull deflection is not absolutely necessary for an array operating at a VHF or lower UHF frequency. Finally, a design of the

demonstration T/R module is proposed. Based on projected communication requirements, the full-scale WNODAR demands a 3.7 Gb/s data transmission rate. The multi-input multi-output orthogonal frequency division multiplexing (MIMO-OFDM) approach has been identified as a promising solution to achieve gigabit transmission rates. To demonstrate and further develop the wireless opportunistic array concept, the following additional research is required:

- The measurement of ship hull deflection while a ship is underway in various sea states for more advanced radar system tradeoff studies;
- The development of signal processing and beamforming software for the WNODAR;
- The demonstration of a low power T/R module based on National Instruments (NI) compact realtime I/O (CompactRIO) modules;
- The anlaysis and simulation of wireless communication for the full scale array.

I. INTRODUCTION

A. MOTIVATION

Weapons of mass destruction (WMD) and the ballistic missiles that deliver them pose a major threat to the security of the United State and its allies. While the end of the Cold War greatly reduced the threat of a global conflict, the proliferation of WMD and ballistic missiles raise new threats to security. Over 20 countries possess or are developing nuclear, biological, or chemical (NBC) weapons, and more than 20 nations have theater ballistic missiles (TBMs) [1].

The ballistic missile defense (BMD) strategy that addresses this threat is shown in Figure 3. A vital component of the strategy is the ability to perform long-range surveillance and tracking of the TBMs upon initial launch. Because of the distributed nature of threats, radar sensors need to be forward positioned to take them closer to the suspected enemy launch sites. Navy ships that perform this role are equipped with conventional large phased array radars (LPAR) with thousands of independent, active array elements to detect and discriminate missile targets from thousands of miles away. The Cobra Dane is a land-based, L-band LPAR at Alaska, with a maximum range of 3000 nm. It can locate an object 10 cm in diameter at range of 2000 nm with an accuracy of 5 m. To do so, the radar needs to generate 15.4 MW of peak radio frequency (RF) power from 96 traveling wave tube (TWT) amplifiers. The power is radiated through 15,360 active array elements, which together with 19,408 inactive elements comprise the 94.5 ft diameter array face, as shown in Figure 4.

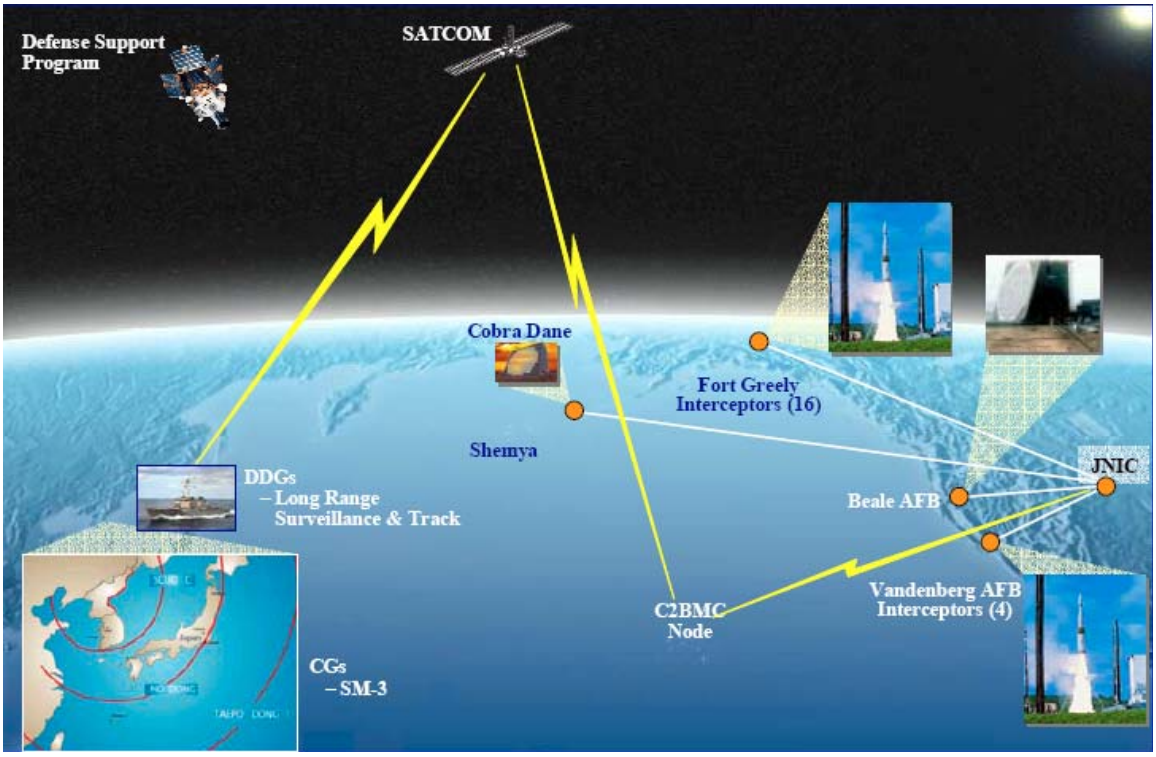

Figure 3. Ballistic Missile Defense Strategy (From [2]).

Figure 4. Cobra Dane LPAR (From [3]).

There are many technical challenges which make the implementation of LPAR difficult. Conventional microwave beamforming using TWTs and analog phase-shifters at every array element is complicated, costly and subject to the calibration and drift issues associated with analog components. The signal distributing network involves hundreds of feet of transmission lines, various switches and coupling networks. Figure 5 shows a conventional high power phased array beamforming network using waveguides. Clearly the volume and weight of such an array is undesirable, especially if it is to be mounted on a ship for forward deployment. For LPARs that physically distort with ship flexure,

element localization and synchronization are predominant issues. Adaptive beamforming is required to calibrate the complex weight at each array element in a way that the distorted array can form a beam in any desired direction.

Figure 5. Waveguide array (Courtesy of Hughes Aircraft).

New antenna concepts and technologies are making dramatic performance improvements to LPAR possible. The "opportunistic array" concept has been the focus of research and development undertaken by the Naval Postgraduate School (NPS). An opportunistic array is an integrated ship wide digital phased array, where the array elements are placed at available open areas over the entire surface of the platform. The elements of the opportunistic array are self-standing digital transmit/receive (T/R) modules with no hardwire connections other than prime power. Element localization and synchronization signals, beam control data, and digitized target return signals are passed wirelessly between the elements and a central signal processor. Hence this approach is more concisely described as a wirelessly networked opportunistic digital array radar (WNODAR).

The opportunistic array concept and digital architecture of the WNODAR are also well suited to the "aperstructures" philosophy [4], where the array is an integrated load-bearing part of the ship structure. This philosophy is being applied to the DD(X)

program and is currently under research and development. Figure 6 shows the Integrated Deckhouse that aims to populate the ship's deck with antennas embedded into the ship's composite superstructure.

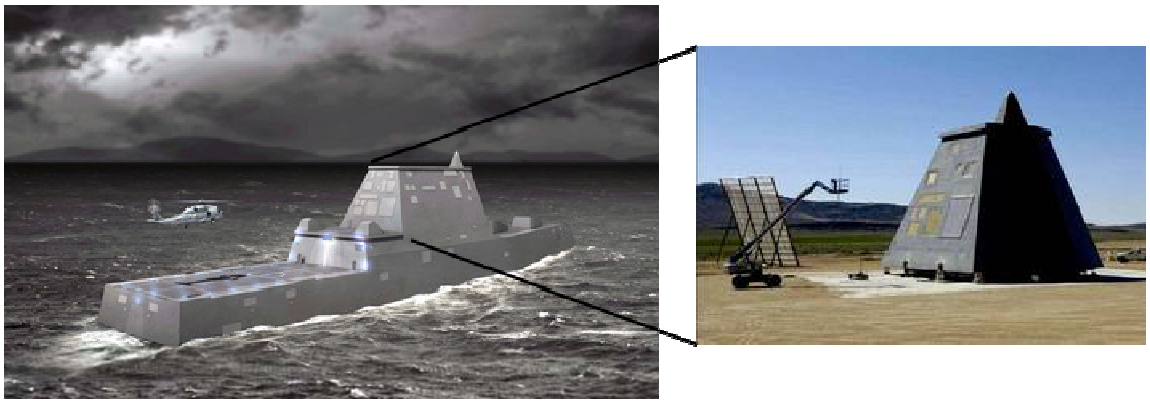

(a) (b)

Figure 6. (a) Artist's concept of the DD(X) and (b) Integrated Deckhouse mock up for antenna and signature testing (From[5]).

The WNODAR has many advantages over the analog LPAR. Firstly, being a digital phased array, it is capable of multiple simultaneous receive beams, rapid dynamic reconfigurability of the various output beams, dynamic null steering, and very low sidelobes through digital calibration. Secondly, the digital architecture eliminates the need for analog beamforming components. Thirdly, the conformal, dispersed element opportunistic array concept using hull appliqués retains the stealth characteristics of the warship, maximizes its survivability and maneuverability, and allows the possibility of economic retrofits.

Previous research at NPS was conducted in the areas of digital phased array architecture, basic radar system tradeoffs and studies related to the design of the individual T/R modules; namely the wireless local oscillator (LO) distribution and control methods, microstrip patch antenna design, and commercial-off-the-shelf (COTS) hardware investigation. A key challenge is the need to perform synchronization of the hundreds or even thousands of array element to provide time and frequency references. Synchronization is required to scan the beam and perform coherent detection and integration. In addition, there is a need to perform dynamic measurement of element locations to correct for errors due to ship hull deflection. Element location data is

required for digital beamforming to avoid degradation in the sidelobes, gain, and beam pointing. This thesis attempts to address the above concerns.

B. THESIS OBJECTIVE

The objective of this thesis is to address the problem of integrating the elements of an opportunistic array through the design of a wireless synchronization and geolocation network. This can be divided into the following tasks. Firstly, this thesis examines possible approaches to dynamically synchronize all of the elements to a common frequency and time reference to overcome the dynamic transmission paths from the central processor to the array elements. Secondly, this thesis presents an analysis of position errors and a survey of suitable geolocation techniques for array elements. The effect of hull deflection on radar performance is simulated to determine the need for accurate and dynamic position sensing. And thirdly, this thesis proposes the design of a demonstration T/R module system, with particular focus on possible wireless communication systems capable of supporting the simultaneous, high data rate transmission of element localization, synchronization signals, beam control data and digitized radar signals.

Synchronization of array elements to a common time and phase reference is required. Previous research has shown that control of the elements' phase is possible via a wireless LO signal, but in a dynamic environment the transmission paths will be changing and unpredictable. To overcome this, two synchronization techniques were studied. Generally, the techniques aim to get phase corrections for synchronization without explicit measurement of the elements' position displacement. Simulation models were used to validate this approach; performance characteristics were established for comparison.

Geolocation of the element positions is crucial in digital beamforming. In a static situation, one-time measurement of every element's location might be sufficient. However, in an opportunistic array the element positions on the ship are continuously changing due to ship hull deflection and this fact must be taken into account in the signal processing to avoid degradation in the sidelobes, gain and beam pointing. An analysis of

position errors and a survey of suitable geolocation techniques were performed. The effect of hull deflection on radar performance was simulated to determine the need for accurate and dynamic position sensing.

Wireless communication has received significant attention in recent years. This has led to improvements in array element design and a wide variety of low-cost, high-performance, radio frequency (RF) circuits that help make digital antenna a cost effective option. Conventionally, the LO signal and signal processing information is provided to each element via microwave transmission line. The desired goal is to replace this with a wireless link that is able to provide gigabit transmission rates between the hundreds or even thousands of elements distributed over the ship surface.

C. THESIS OUTLINE

This thesis is organized as follows. Chapter II describes the WNODAR system architecture and the key components of the individual T/R module. Previous work completed on the WNODAR is summarized. The challenge to synchronize array elements is discussed and the communication architecture to address this challenge is proposed. The subsequent chapters present the key components of the communication architecture. Chapter III examines possible approaches to dynamically synchronize array elements to a common time and phase reference. Simulation was used for analysis and comparison. Chapter IV presents a technical survey of geolocation techniques for array elements, and an analysis on the effects of ship hull deflections on radar performance. Chapter V proposes the design of a demonstration T/R module to validate the wireless opportunistic array concept. The solution to gigabit transmission rates using commercially available wireless communication systems is discussed. Finally, Chapter VI summarizes the work in this thesis and offers suggestions for future research.

II. SYSTEM ARCHITECTURE FOR THE WNODAR

This chapter describes the system architecture for the WNODAR and the key components of the array elements comprising individual T/R modules. This is followed by a summary of the previous work completed on the WNODAR. The challenge to synchronize array elements is discussed and the communication architecture to address this challenge is proposed.

A. SYSTEM OVERVIEW

An opportunistic array is an integrated ship wide digital phased array, where the array elements are placed at available open areas over the entire length of the platform. The elements of the opportunistic array are self-standing digital T/R modules with no hardwire connections other than prime power. Element localization and synchronization signals, beam control data, and digitized target return signals are passed wirelessly between the elements and a central signal processor. This approach can be described as a wirelessly networked opportunistic digital array radar (WNODAR).

Figure 7 shows the WNODAR deployed on a DD(X) type platform and the simulated antenna pattern for a 1200 element array performing a broadside scan. Depending on the scan direction, not all elements are active. For example, only 620 active elements need to contribute to a broadside scan. Active elements are those with nonzero aperture area facing the scan direction. From the results of system level tradeoff studies, the key operating parameters for the WNODAR are summarized in Table 1. For BMD applications, the WNODAR operates at 300 MHz in the upper VHF or lower UHF band. Rain and atmospheric attenuation are negligible, and the Doppler frequencies of the targets of interest are sufficient. Operating at this frequency allows elements to be spaced up to a meter, and phase errors due to the physical displacements of the elements that arise from ship surface distortion are not large in terms of wavelength.

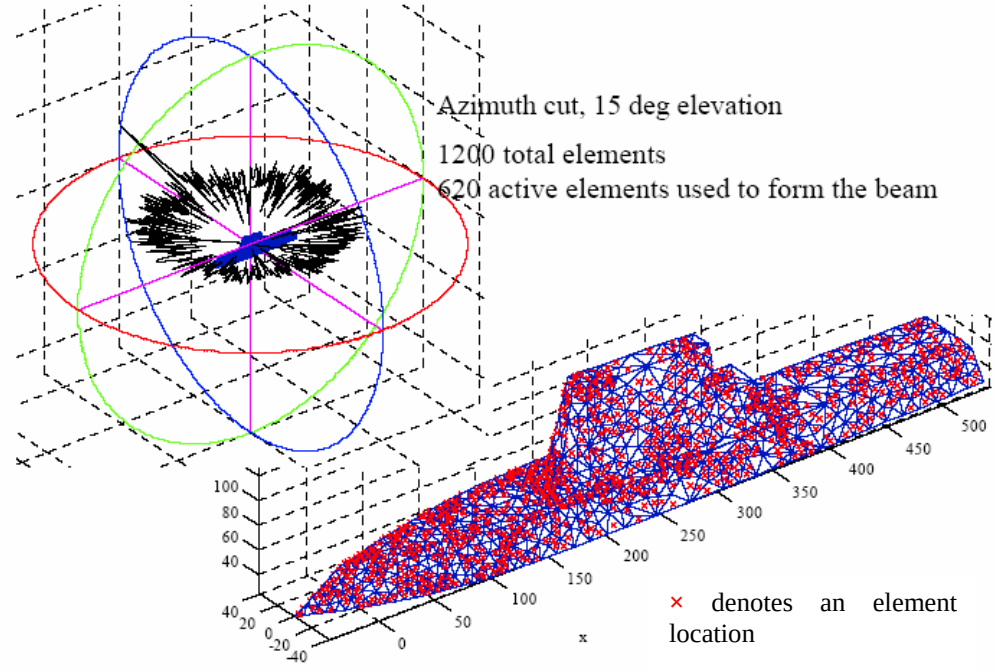

Figure 7. Simulated array pattern and ship model (dimensions in feet) (From [6]).

Parameter	Specification
Operating frequency	300 MHz
Number of elements	1200
Detection range for 10 m^2 target	2000 km
Average power per element	500 W
Beamwidth	0.31°
Pulse width	16 ms
Duty cycle	0.25

Table 1. Key operating parameters for the BMD WNODAR.

B. SYSTEM ARCHITECTURE

A basic block diagram of the WNODAR system architecture is shown in Figure 8. For clarity, only a single T/R module and array element is shown. The WNODAR comprises of the central digital beamformer and controller that communicates wirelessly with hundreds or even thousands of array elements that are self-standing T/R modules. For a ship application, the central digital beamformer and controller can be located below deck, while the array elements are randomly distributed over the platform surfaces.

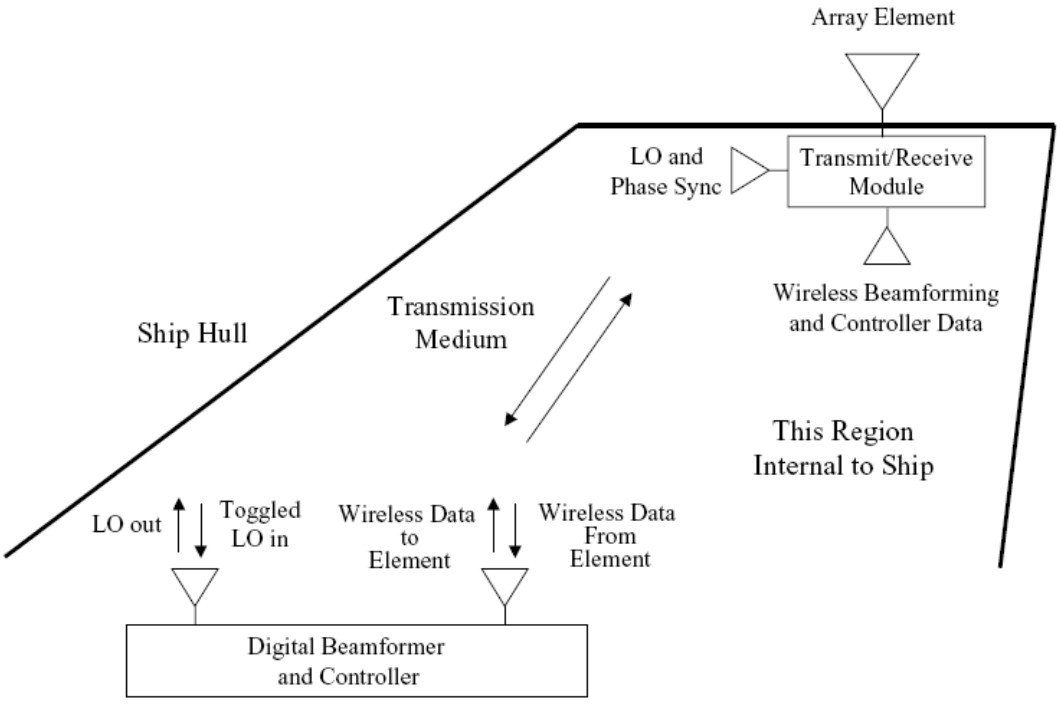

Figure 8. System architecture for the WNODAR (From [6]).

The general operational concept of the WNODAR is as follows. The central digital beamformer and controller computes the beam control data (phase and amplitude weights for each element) and radar waveform parameters. These are combined with the LO and synchronization signals and are passed wirelessly to all array elements.

A detailed architecture for each T/R module is shown in Figure 9. At each array element, the digital baseband signal is generated by the direct digital synthesizer (DDS), converted to analog (with the D/A), directly up-converted to the operating band and power amplified. On receive, the signal is downconverted to baseband after low-noise amplification, quantized (with the A/D) and the in-phase and quadrature data returned to the central digital beamformer and controller for processing. The LO reference signal is distributed wirelessly. An active phasing technique is used to compensate for element dynamic position changes and propagation channel changes.

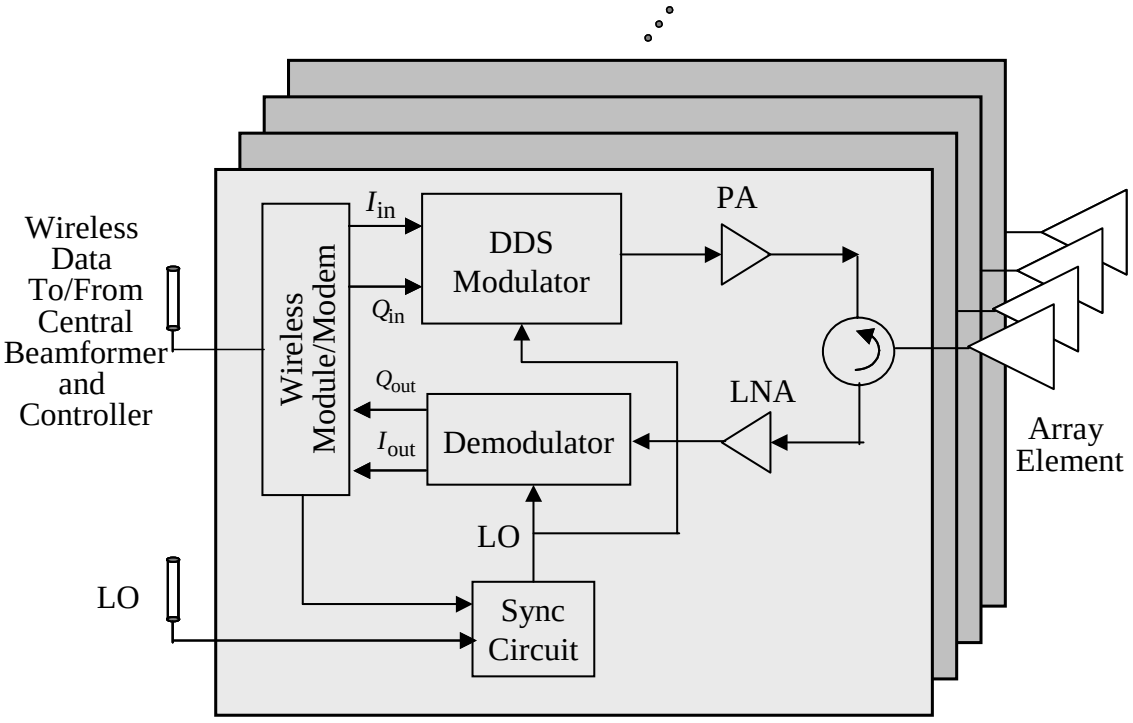

Figure 9. System architecture for the T/R module (From [6]).

C. SUMMARY OF PREVIOUS WORK

1. Design of Digital Array Radar

The first phase of research into the opportunistic array concept and the WNODAR at NPS led to the design of a digital transmit antenna with hard-wired array elements that operate from 2 to 2.5 GHz. In [7], a three-dimensional 2.4 GHz test-bed phased array transmit antenna was constructed using COTS products. The antenna was constructed using the Analog Devices AD8346EVAL quadrature modulator boards, which were assembled into a 24-element array and configured as phase shifters. The formation of the radiation beam with randomly located elements was verified to be in agreement with computer simulations using the Genetic Algorithm (GA), demonstrating the viability of the transmit component of the phased array. The GA has advantages in pattern formation for cases where the array geometry is random or aperiodic.

In [8], the research investigated the bandwidth characteristics of the AD8346EVAL modulator board. Another commercial product, the Analog Devices AD8347EVAL quadrature demodulator board was configured to operate as a receive

phase shifter, and the phase response from the demodulator was measured and compared against the transmit phase from the modulator. Reference [9] investigated the design of the complementary phased array receiver architecture using the AD8347 demodulator. To improve the phase distortion and increase the operating bandwidth of the phased array, the technique of using different types of time-varying phase weights for a linear frequency modulated signal was demonstrated for the transmit side.

2. Basic Radar System Tradeoffs

In order to perform the BMD mission, the antenna gain and other radar system parameters must be capable of detecting targets out to 1000 km or more. In the second phase of research, a system level tradeoff was performed to size the system and verify that this detection range could be achieved. A CAD model for a DD(X) sized ship was built and various numbers of array elements distributed randomly over the ship platform as shown in Figure 7. Using the values of gain determined for various numbers of elements, the relationship between the theoretical maximum range and the total number of antenna elements was determined.

From the simulation results [10], assuming that each element delivers an average power of approximately 500 W, only 400 elements are required to achieve a theoretical maximum range of 1000 km. If 800 elements are available, a theoretical maximum range of approximately 1600 km is possible. If 1200 elements are available, a theoretical maximum range beyond 2000 km is possible. In addition, a low-profile, broad-band U-slot microstrip patch antenna that could operate in the upper VHF/lower UHF frequencies was designed for the array elements. A set of simple design procedures was proposed to provide approximate rules that result in a good “first-pass” design with prescribed characteristics that require minimal tuning.

3. Wireless LO Signal Distribution and Transmission System

Distribution of the LO signal is a requirement for coherent operation of the array elements. In [11], a laboratory demonstration of the wireless LO was successful, paving the first step towards a fully wireless opportunistic phased array. A sinusoidal LO signal was transmitted, and then received by two AD 8346 modulator boards operating at 2.4

GHz. It was also shown that control of the elements' phase is possible via a wireless LO signal. Also in [11], investigations into the possible transmission systems for the aperstructure indicated that a two-dimensional cylindrical wave structure would incur significantly less power spread loss relative to three-dimensional spherical wave propagation. Parallel plate and grounded dielectric slab transmission systems were investigated. Both had very low loss but the field outside of the dielectric layer can couple with external objects. A completely enclosed transmission structure like the parallel plates is more immune to interference and generates less electromagnetic interference (EMI).

4. COTS Hardware Investigation

Several critical aspects of the opportunistic array concept were demonstrated using COTS hardware in the 2.4 GHz band. Low cost, high-performance modulators and demodulators are available at this frequency. References [7]-[11] demonstrated wireless synchronization of multiple modulator boards (AD8346) and demodulator boards (AD8347), as well as the digitization of demodulator signals (using NI5112 digitizers) that is a necessary step in processing the radar returns. In [12], the feasibility of using the AD 9854 direct digital synthesizer (DDS) board to generate the baseband radar waveform was demonstrated. Methods of generating frequency modulated continuous wave FMCW waveforms and pulsed waveforms from the digital transmit module were investigated. It also examined the necessary adaptations such as up-converting baseband signals from DDS to a radar transmission frequency, viable transmit and receive waveforms and the synchronization problem relating to synchronizing the hundreds or even thousands of radiating elements.

A persistent technology challenge arising from the development of the opportunistic array concept and the WNODAR has been the need to perform synchronization of the array elements to provide time and frequency references. Synchronization of the LO signal and DDS in the T/R modules is crucial for coherent modulation/demodulation of the radar waveforms.

The existing means of synchronizing modulator/demodulator and DDS of the test bed digital antenna involves a delicate process of distributing the reference signal to each individual device without incurring any phase differences between them. But based on results of the system tradeoff studies, hundreds or even thousands of T/R modules will need to be synchronized. In [12] it was reported that *Analog Devices* has recently released a new range of DDS (AD9958-AD9959) that has built-in self-synchronization feature. This new method of synchronization provides the ability to connect these DDSs in a daisy chain that allows clusters of DDSs to be synchronized. In addition, this feature could potentially be used to generate the LO signal at the element if a synchronization signal (trigger) is provided.

D. COMMUNICATION ARCHITECTURE

In order to provide synchronization, it is necessary to design a wireless synchronization and geolocation network to integrate the elements throughout the opportunistic array. The proposed communication architecture is shown in Figure 10.

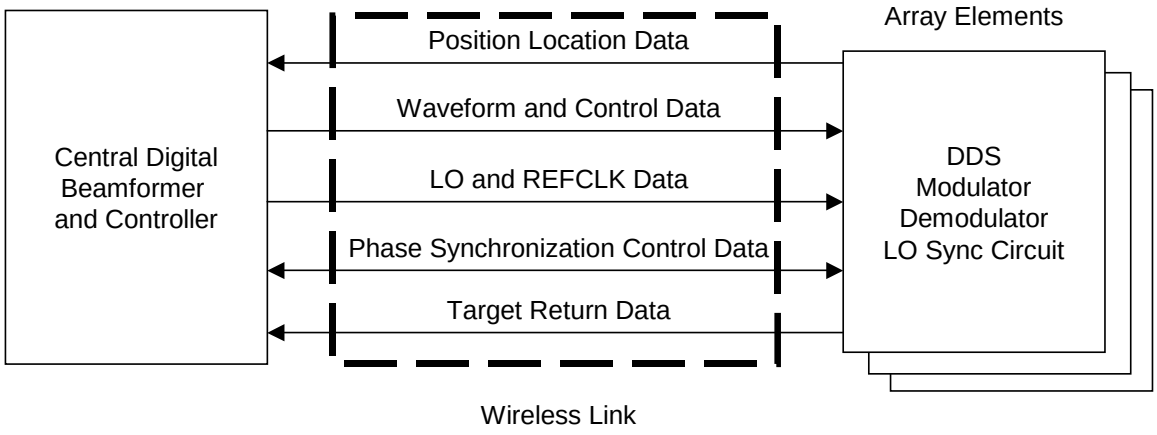

Figure 10. Communication architecture for the opportunistic array.

A broad description of the various components is as follows. At regular intervals, each array element will send its Position Location Data to the central digital beamformer and controller. With knowledge of the element locations, the processor calculates the appropriate digital amplitude and phase weights for each array element for digital beamforming, and broadcasts this information to all array elements in the Waveform and

Control Data. The distribution of the LO (required by the modulator and demodulator) and the REFCLK (required for the DDS) signals is combined into a single waveform. A pulse train is transmitted from the centralized controller and the pulse train envelope detected and used for timing. The carrier can be extracted and used for the LO. Each T/R module will incorporate hardware (LO Synchronization Circuit in Figure 9) for performing the synchronization. The Phase Synchronization Control Data will be used to phase synchronize all the array elements. The amplitude and phase corrected waveform is then modulated, amplified and transmitted. On receive, echo signals are demodulated and the Target Return Data sent to the central digital beamformer and controller for processing. All data communication will be enabled by a wireless link with the capacity to network the entire opportunistic array.

E. SUMMARY

This chapter described the system architecture for the WNODAR and the key components of the individual T/R module. Previous work completed was summarized. The challenge to synchronize array elements was discussed and the communication architecture to address this challenge was proposed. The subsequent chapters present the key components of the communication architecture, namely the options for element synchronization, position location techniques and the technology survey of wireless links capable of gigabit transmission rates.

III. ELEMENT SYNCHRONIZATION FOR THE WNODAR

A persistent technology challenge arising from the development of the opportunistic array concept and the WNODAR has been the need to perform synchronization of the array elements to provide time and frequency references. Synchronization of array elements to a common reference is required to scan the beam and perform coherent detection and integration. Control of the elements' phase is possible via a wireless LO signal, but in dynamic conditions the transmission paths will be changing and unpredictable. To overcome this, two different synchronization techniques are presented in this chapter. Possible hardware architecture for synchronization is presented. MATLAB was used to simulate and evaluate the synchronization techniques. The results and performance characteristics of various approaches are discussed.

A. ELEMENT SYNCHRONIZATION

Synchronization of array elements in time and frequency ensures that the emissions from all elements converge coherently on the target, increasing average power and signal-to-noise ratio (SNR). In each T/R element, the use of a DDS, modulator and demodulator requires precise phase-synchronization of multiple synthesized RF output signals to one another for coherent detection and integration. Quadrature upconversion shown in Figure 11 is used to upconvert the baseband in-phase and quadrature DDS signals to the transmission frequency. In [12], it was shown that amplitude and phase errors create imbalances in I and Q signals, resulting in LO feedthrough and poor sideband suppression.

For our application, frequency is synchronized by a common wireless LO signal, and therefore the key focus is to provide time or phase synchronization. The techniques to provide phase synchronization are examined in the following sections.

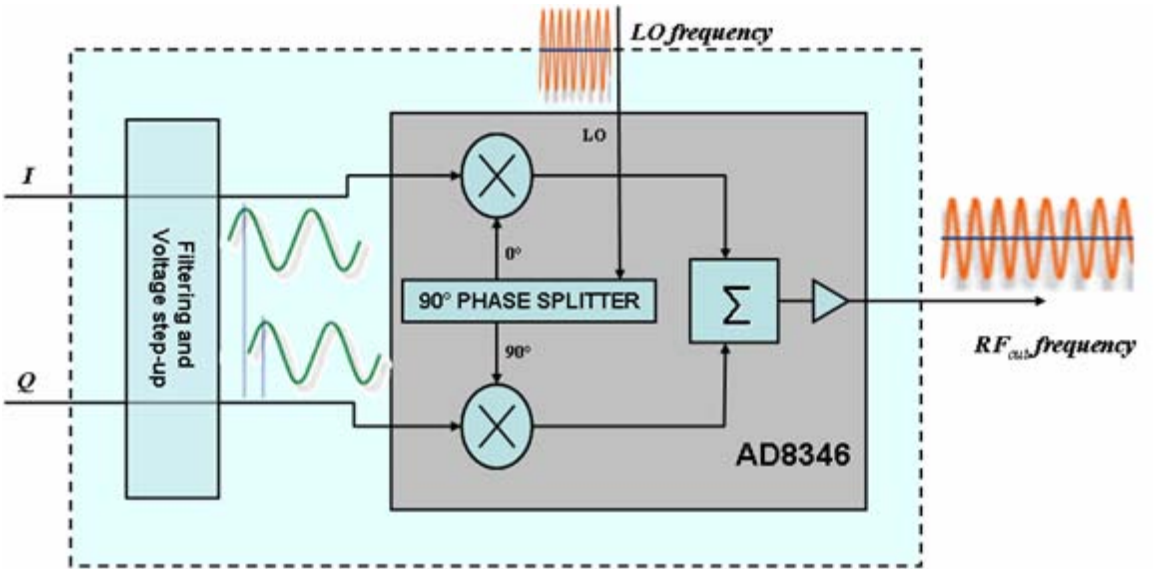

Figure 11. Quadrature upconversion using the AD8346.

B. "BRUTE FORCE" SYNCHRONIZATION TECHNIQUE

1. Concept

The "brute force" synchronization technique is a systematic adjustment of the array element phases. It is easy to implement with some hardware incorporated in each array element and in the central digital beamformer and controller. Figure 12 shows a detailed diagram of the synchronization block that is required in each array element. Each synchronization block comprises a modem and controller connected to a phase shifter and a switch. When the switch is positioned for synchronization operation (as shown) the LO signal is passed through a circulator, low-noise amplifier (LNA), phase shifter and then retransmitted back and compared to a reference signal at the central controller. Under normal operation (switch opposite as shown), the LO signal is sent out to the modulator and demodulator for coherent beamforming.

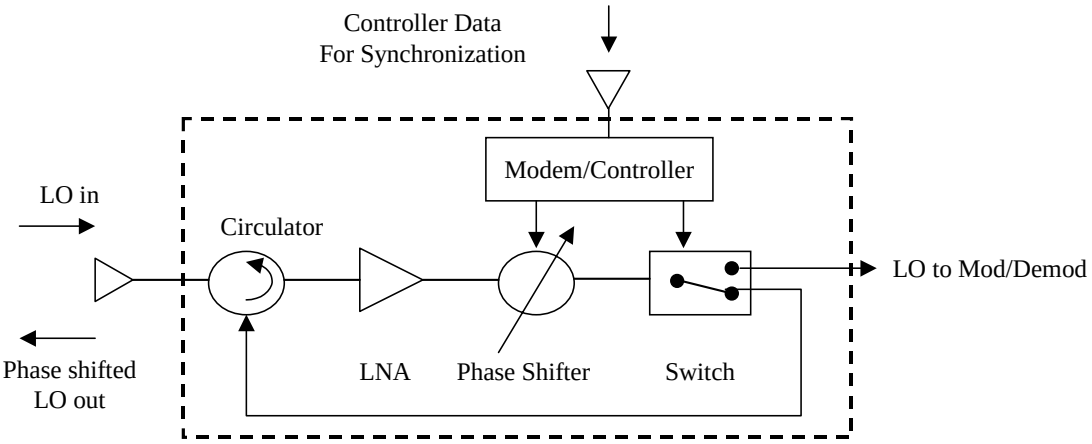

Figure 12. Diagram of a synchronization block for one element (From [13]).

Figure 13 shows the general concept to perform phase synchronization for element *n*. The LO signal from the central controller arrives at the synch block of each element at a different phase, given by e^{-jkr_n}, where k is the wave number and r_n is the distance from the central controller to the element *n*. One element is selected as the reference element and it receives the corresponding LO signal $e^{-jkr_{ref}}$. The objective is to synchronize all the elements to the reference element by adjusting the phase shifter ϕ_n to correct for the difference in path length $\left(r_{ref} - r_n\right)$.

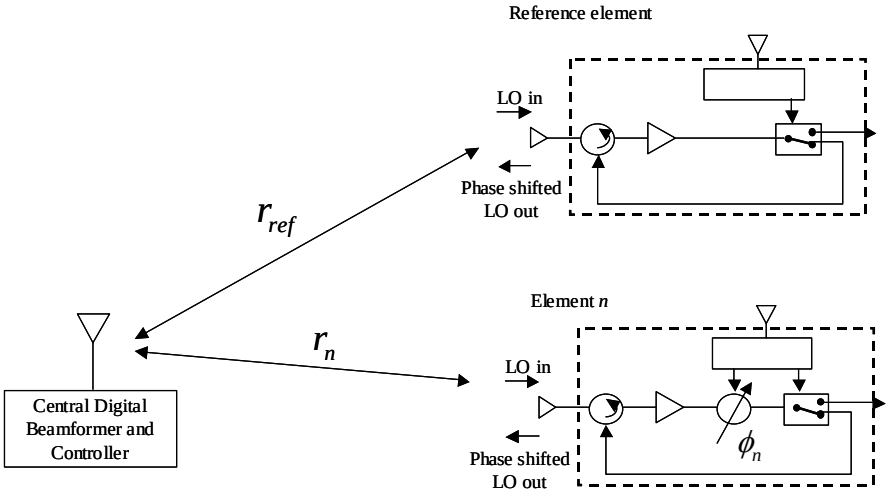

Figure 13. Phase synchronization using the "brute force" technique (After [13]).

At the start of the synchronizing cycle, the central controller sends out each element's address in turn. When the element is selected, the switch is selected to the synchronization position, the received LO signal is shifted by ϕ_n and sent back to the central controller. At the central controller, the LO signal from element *n* is compared with the received LO signal from the reference element. Assuming the amplitudes are suitably compensated by signal amplifiers, the combined field at the central controller is given by

$$\begin{aligned} E_{difference} &= E_n - E_{ref} \\ &= e^{-j(2kr_n+\phi_n)} - e^{-j(2kr_{ref})} \end{aligned} \tag{3.1}$$

where

E_n is the field from element *n*

E_{ref} is the field from reference element

Phase shifts ϕ_n are introduced in element *n* until the two signals cancel. The element and reference signal will cancel when $\phi_n = 2k\left(r_{ref} - r_n\right)$. When ϕ_n is known, the difference in path length $\left(r_{ref} - r_n\right)$ can be corrected and all the elements can be synchronized. This method will also correct for any phase variation due to differences in the propagation channels (e.g., walls with different insertion phases).

2. Simulation

Computer simulation in MATLAB was performed to verify the "brute force" technique. Program *brute_force.m* was used to phase synchronize a WNODAR with 100 elements, distributed randomly over the CAD model of a DD(X) type ship, as shown in Figure 14. The CAD model has 2091 faces, 100 faces were randomly selected and the elements were located at the center of each face. The central controller was arbitrarily located at the origin, so that the transmission path length is equal to the norm of the *x*, *y*, and *z*, coordinates of element *n*.

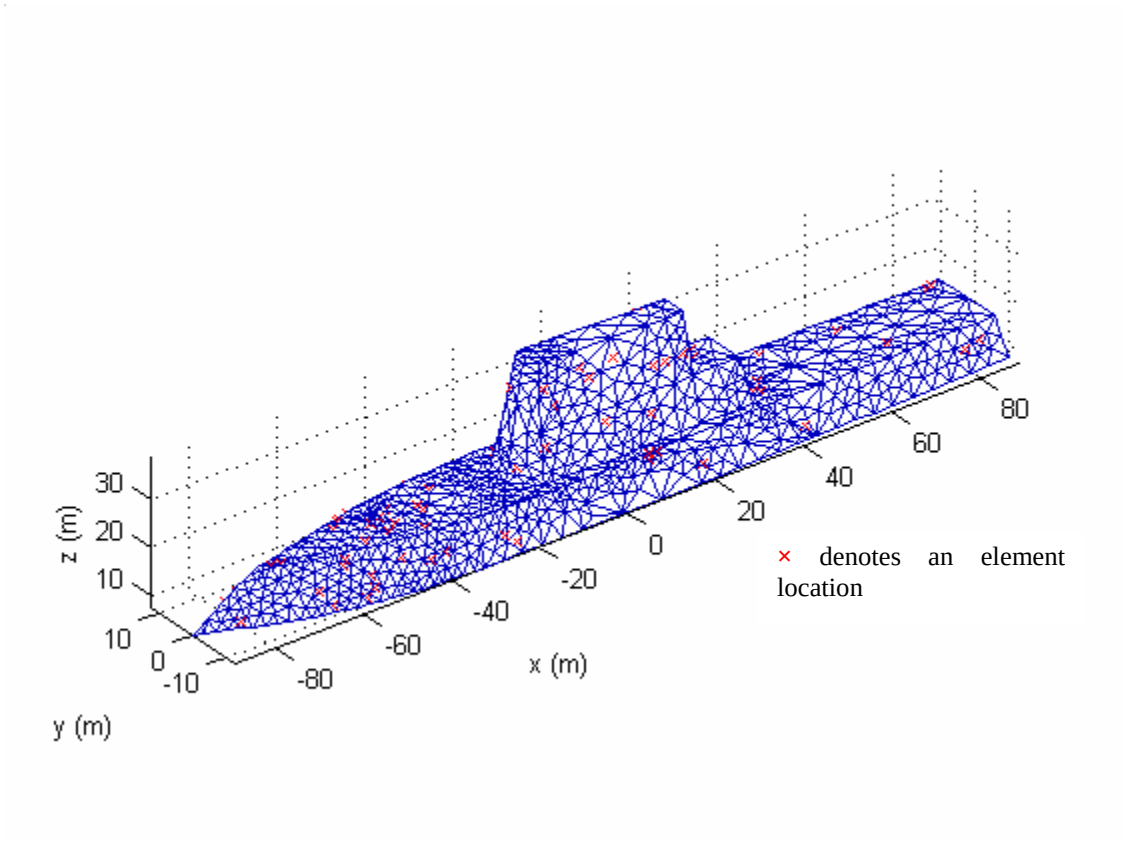

Figure 14. DD(X) model with 100 randomly distributed elements.

Program *brute_force.m* functions as follows. All elements are initialized with zero phase and the element closest to the origin is selected as the reference element. Each element is selected in turn for synchronization. When the element is selected, its phase shifter is incremented in 22.5° steps (equivalent to four-bit digitization) until the combined field is minimum. This is then repeated for the rest of the elements. Four-bit digitization is deemed satisfactory for digital phase shifter quantization based on the required sidelobe level [14]. An analysis on the effects of digitization is covered in Section D of this chapter.

Figure 15 shows the phase error of each element from the reference element plotted against the number of iterations. A change in color denotes a new element being synchronized. For one realization of the 100 randomly located elements, 872 iterations were required to perform synchronization.

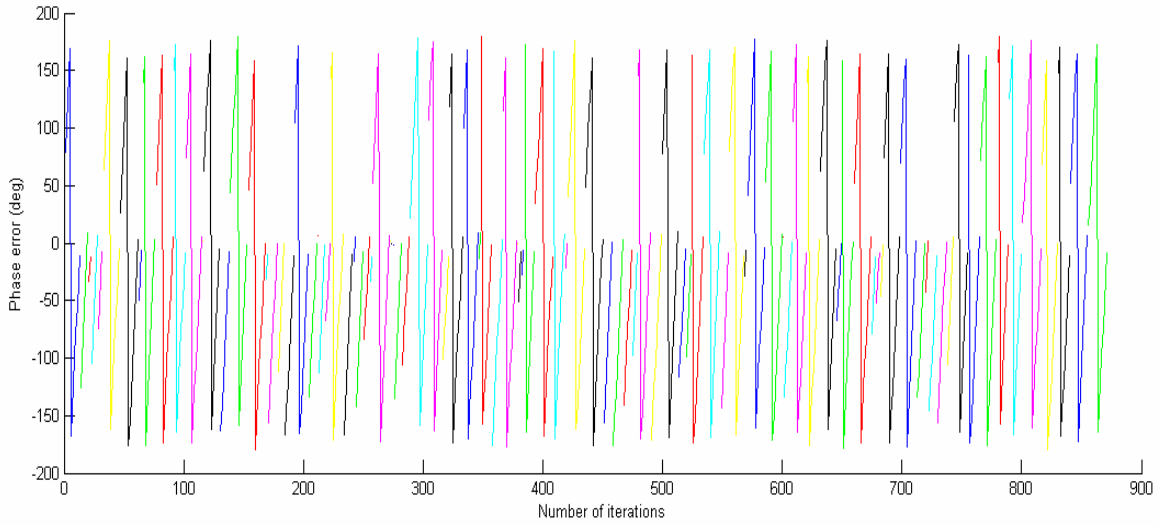

Figure 15. Phase synchronization using *brute_force.m.*

For fixed phase steps, it is not possible to achieve complete cancellation. Therefore program *brute_force.m* requires a threshold value to detect the minima when the two signals cancel. Assuming equal amplitudes and using $22.5°$ steps, the final phase error is $\pm 11.25°$. The minimum field can be computed using phasor geometry

$$\begin{aligned} \min\left(\left|E_{difference}\right|\right) &= \left|E_{ref}\, e^{-j(11.25°)} - E_{ref}\right| \\ &= 2\sin\left(11.25°/2\right) \\ &= 0.196 \end{aligned} \tag{3.2}$$

Hence, a threshold of 0.2 (–14 dB) is used to determine the minima. With 16 phase steps between 0 and $360°$ about eight iterations on average were required to synchronize each element. When the elements are co-phased with the reference element, the final phase error is between $\pm 11.25°$, as shown in Figure 16.

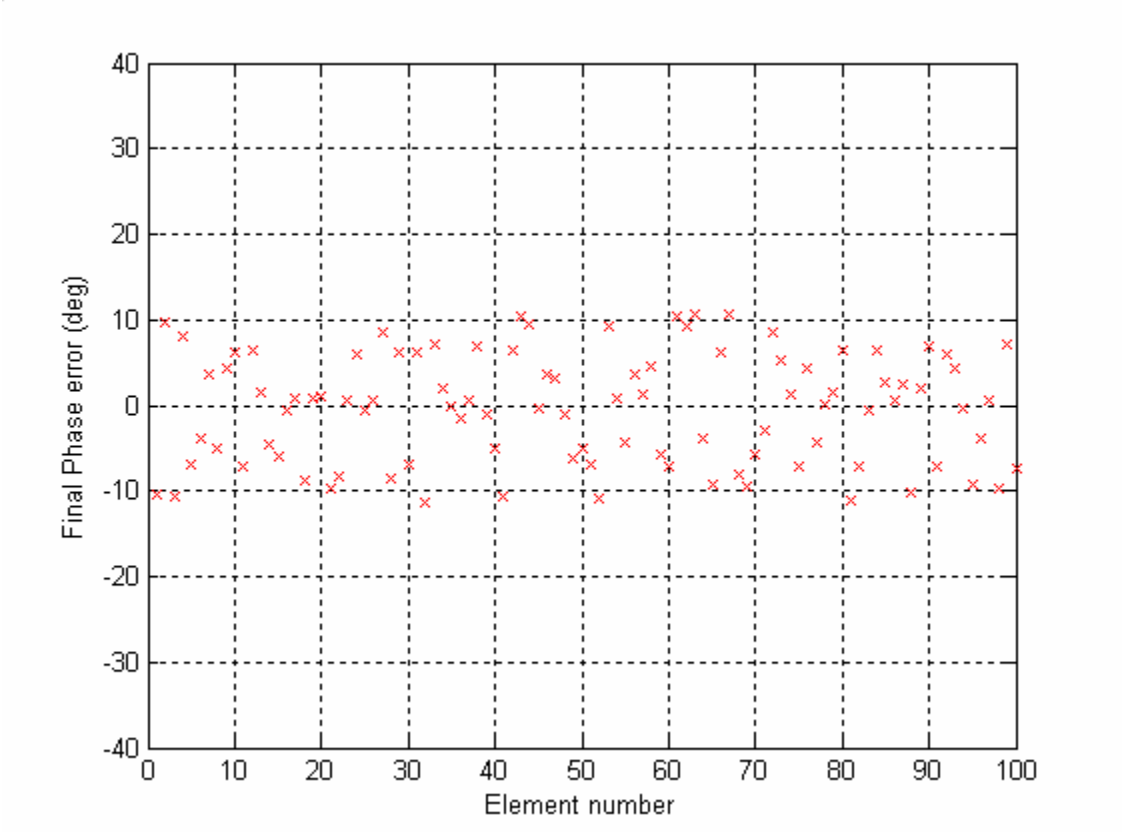

Figure 16. Final phase error using *brute_force.m*.

3. Discussion

On average, the "brute force" technique requires half the total number of quantization levels to synchronize one element because the required phase shift is unknown. This situation can be improved. In our application, the element locations are accurately surveyed during installation. This can be used to provide a good initial phase correction instead of initializing to zero phase. The synchronization technique is then used to correct dynamic changes in the transmission path length, which are relatively small changes that are a fraction of a wavelength. As a result, relatively coarse phase corrections spanning the range of $\pm 20°$ may be sufficient. Just two bits (representing $+10°$, $-10°$, $+20°$ and $-20°$) are required in the synchronization circuit. With PIN diode phase shifters, switching of two bits can be done between 1 ns to 2 ns per element. For the full scale 1200 element array, synchronization can be done in about $2\mu s$ to $3\mu s$.

An issue that has not been addressed is whether phase correction or synchronization at a single frequency is sufficient. A single frequency is sufficient for

simple waveforms such as continuous wave (CW) or narrow band pulsed CW operation. For more complicated wide band waveforms that employ frequency modulation, frequency hopping or pulse compression techniques, synchronization may have to be carried out at several frequencies or at the center of a band of frequencies. This will add more complexity to the synchronization hardware and software requirements. Further investigations will have to be carried out in this area.

C. "BEAM TAGGING" SYNCHRONIZATION TECHNIQUE

1. Concept

"Beam tagging" is proposed in [15] for self-focusing or steering of an adaptive transmitting array. It is a technique of applying low-index phase modulation to one of two antennas aimed at the same target, and measuring resultant amplitude modulation to correct the phase alignment between them. This technique has been used to phase-align lasers onto a target and for testing a large radar array [16].

The "beam tagging" technique can be implemented with more hardware modifications. Figure 17 shows the proposed synchronization system. The key changes are the addition of a phase modulation circuit on the element synchronization block and an amplitude modulation (AM) receiver circuitry on the central controller. In each element synchronization block, the modem controller holds a phase shift command and is able, on special request, to modulate the phase rapidly by ±90° from the command phase, as driven by a square waveform generator.

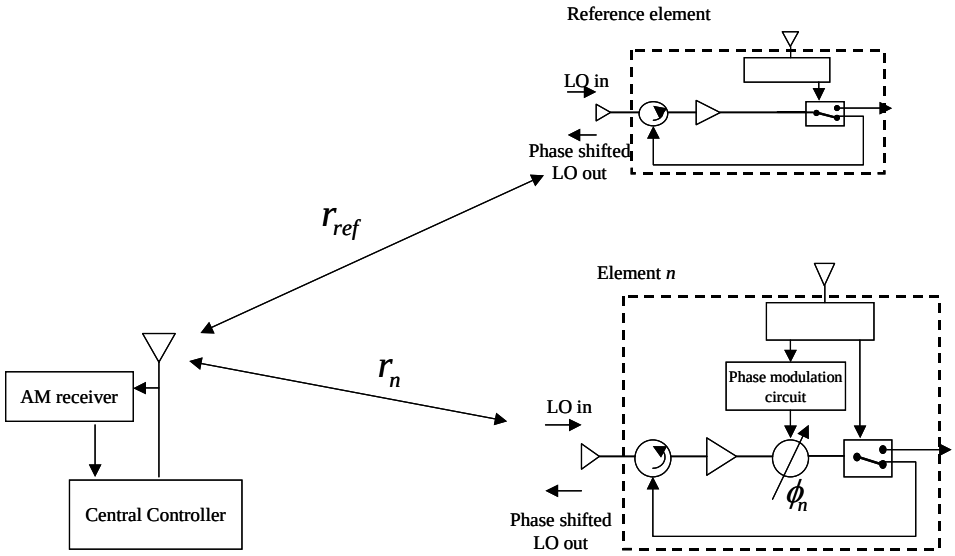

Figure 17. Phase synchronization using the "beam tagging" technique.

The general operational concept is as follows. When element *n* is selected by the central controller, the phase shifter phase modulates its LO output by $\pm 90°$ and sends it back to the central controller. This phasor signal is compared with the combined field E_{sum} ($E_{sum} = E_n + E_{ref}$), as shown in Figure 18. If element *n* is producing a field E_n which is normally in phase with the reference element field E_{ref}, then moving its phase $90°$ ahead and $90°$ behind reduces the combined fields $E_{sum}^{+90°}$ and $E_{sum}^{-90°}$ to an equal extent. However, suppose the field E_n leads E_{ref} by $\Delta\theta$. Then advancing the phase decreases the total field, and retarding the phase increases it. This rapid modulation of the element LO produces a corresponding amplitude modulation of the field. This AM signal is used as a feedback control mechanism for synchronization.

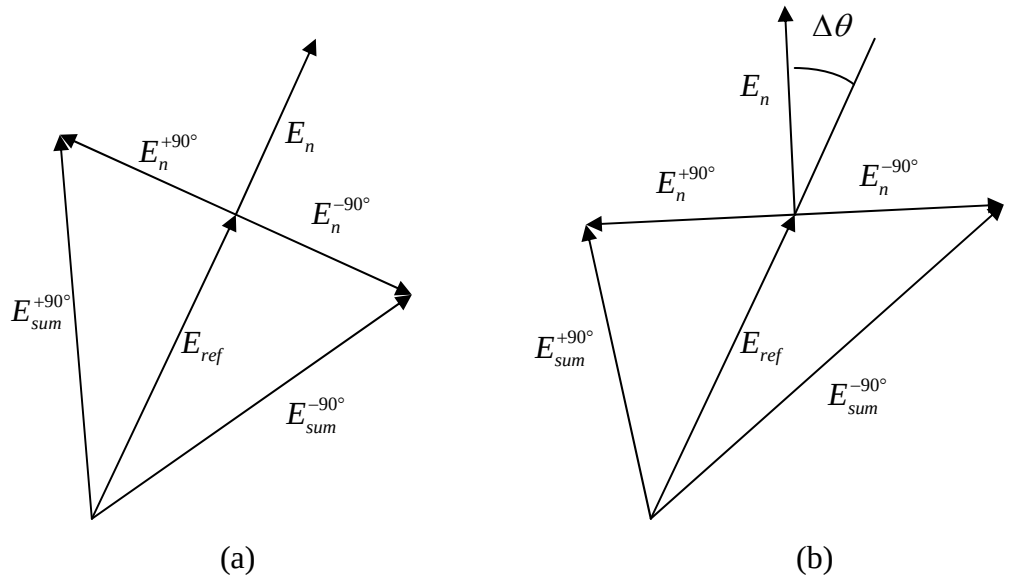

(a) (b)

Figure 18. Phasor diagrams (a) element *n* in phase (b) element *n* leading.

At the central controller, the amplitude of the AM signal is detected and compared with the phase of the LO modulation which serves as a reference. When $0 < \Delta\theta < 180°$ then $E_{sum}^{+90°} < E_{sum}^{-90°}$, the phase correction circuit decreases ϕ_n. Conversely, when $180° < \Delta\theta < 360°$ then $E_{sum}^{+90°} > E_{sum}^{-90°}$, the phase correction circuit increases ϕ_n. Two balance conditions occur at $\Delta\theta = 0$ and $\Delta\theta = 180°$. The desired balance condition $\Delta\theta = 0$ is stable, whereas at the other balance condition when $\Delta\theta = 180°$, any small change in $\Delta\theta$ brings it back to the stable balance condition.

2. Simulation

Simulation was performed to verify the "beam tagging" technique based on the same initial conditions used earlier. Two variations, *beam_tag1.m* and *beam_tag2.m* were tested using different approaches to arrive at the balance condition. In program *beam_tag1.m*, phase corrections are performed until an opposite command is detected. This means that the element phase relative to reference has changed from lead to lag or vice versa and balance condition is reached. Program *beam_tag1.m* detects this and terminates the synchronization cycle.

Figure 19 shows the phase error of each element against the number of iterations. The program *beam_tag1.m* synchronized the array after 546 iterations, a significant reduction of 38% in the number of iterations. The steady phase error is between $\pm 22.5°$ (see Figure 20). The steady phase error is greater because when the synchronization cycle is terminated, the phase could have been overcorrected by $22.5°$, giving rise to the error of $\pm 22.5°$.

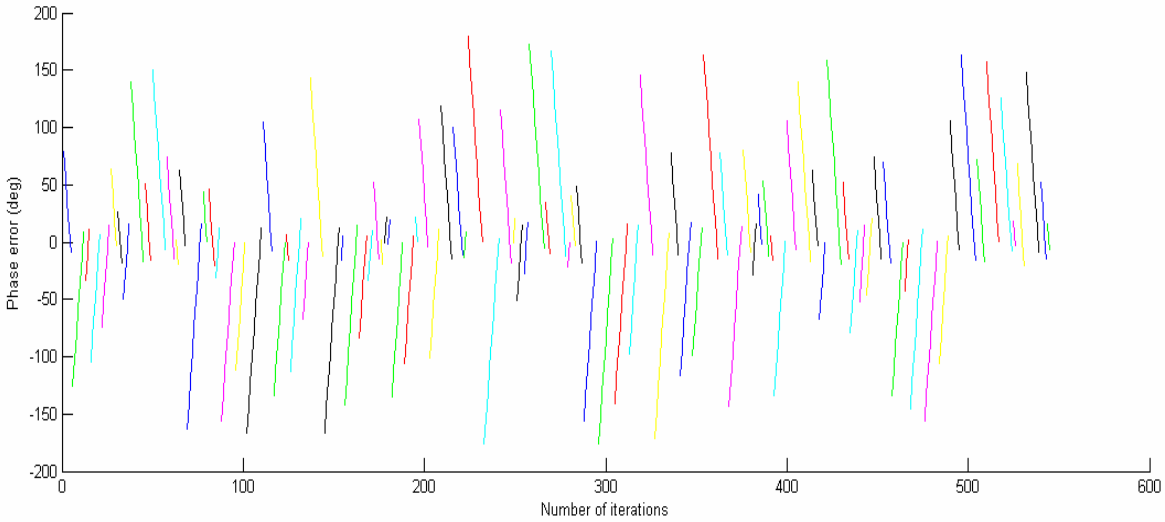

Figure 19. Phase synchronization using *beam_tag1.m*.

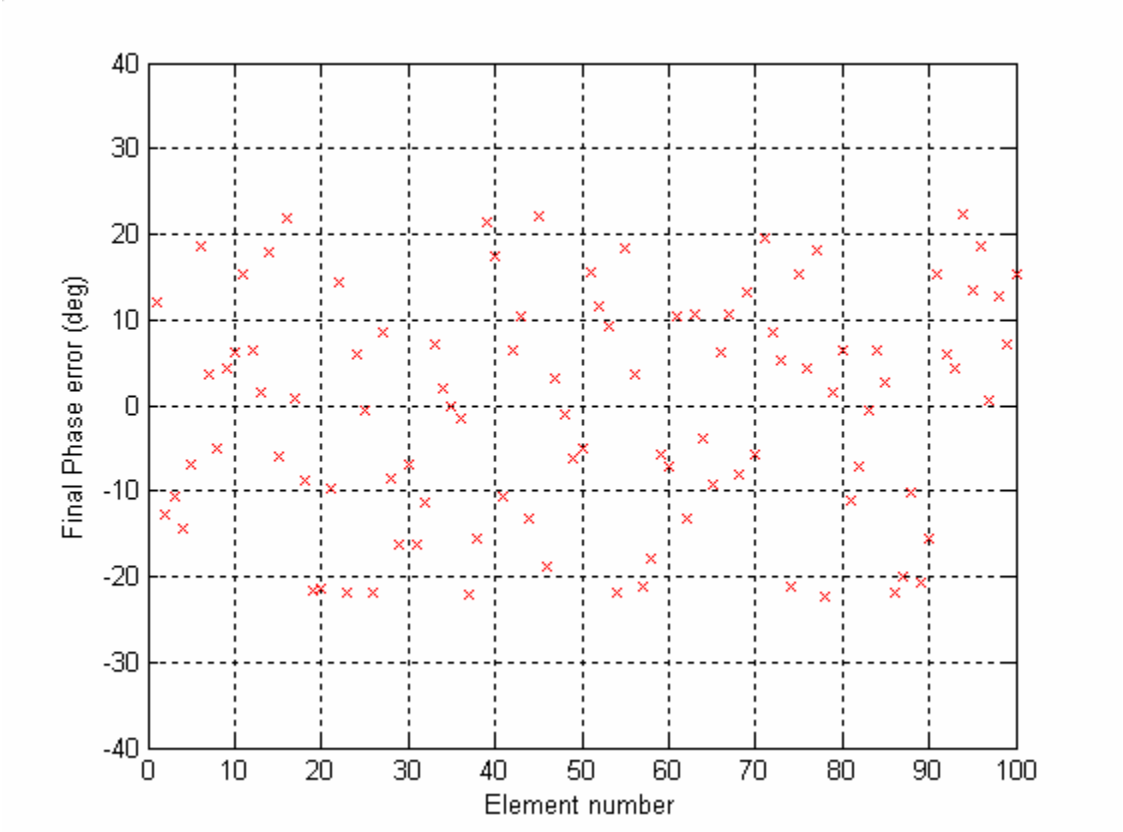

Figure 20. Final phase error using *beam_tag1*.

It is possible to reduce the final phase error at the expense of the number of iterations by introducing the following test mechanism. In program *beam_tag2.m*, the amplitudes $E_{sum}^{+90^\circ}$ and $E_{sum}^{-90^\circ}$ are compared at the two states near the balance condition. Since a greater $\Delta\theta$ increases the amplitude of the modulation, program *beam_tag2.m* selects the phase correction that gives the lower amplitude. Using Figure 18, it can be calculated that the amplitude modulation for $\Delta\theta = 11.25^\circ$ is 0.277 (11 dB), which should be measurable in practice. An additional iteration is then required to reverse the previous command if there is an over correction. Simulation shows that *beam_tag2.m* produces the same results as program *brute_force.m* after 691 iterations.

3. Discussion

Table 2 compares the three synchronization programs. The "beam tagging" technique using *beam_tag2.m* is able to synchronize elements more quickly without

increasing the steady phase error. However, since the synchronization time is on the order of 2 to 3 μs, the improvement is marginal. Based on this consideration, the more simple "brute force" technique is sufficient.

Program	Number of iterations per element	Steady phase error
brute_force.m	8.72	±11.25°
beam_tag#1.m	5.46	±22.5°
beam_tag#2.m	6.91	±11.25°

Table 2. Comparison of synchronization programs.

D. EFFECT OF VARYING SIGNAL AMPLITUDES

1. Concept

In a real environment, the LO signals are subject to attenuation due to transmission loss. The effect of varying signal amplitudes on the synchronization techniques is analyzed. If path loss is taken into account for the LO signal, $E_{difference}$ of Equation (3.1) is replaced by

$$E_{difference} = \frac{1}{2r_n} e^{-j(2kr_n+\phi_n)} - \frac{1}{2r_{ref}} e^{-j(2kr_{ref})} \tag{3.3}$$

Electric field strength is inversely proportional with distance. The effect of varying signal amplitude is significant for elements located far away from the reference element. The distribution of elements shown in Figure 14 has a minimum distance of 17 m, and a maximum distance of 88.8 m. Based on these distances, the relative signal amplitude could vary up to five times.

2. Simulation

Computer simulation shows that the "brute force" technique has limitations when path loss is taken into account. From Figure 21, only about 10% of the elements could be synchronized using the "brute force" technique. On the other hand, the "beam tagging" technique is able to synchronize all elements to the minimum phase error of $\pm 11.25°$.

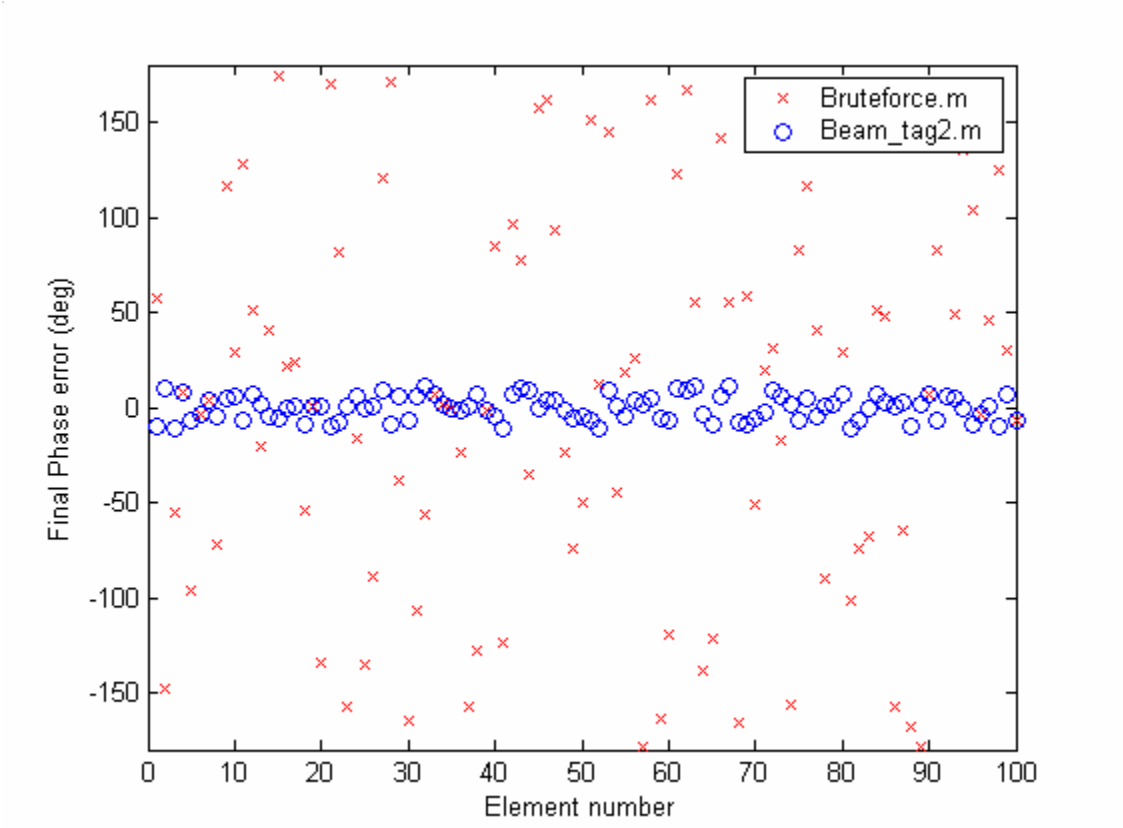

Figure 21. Steady phase errors with the effect of amplitude variation.

3. Discussion

Simulation shows that varying signal amplitudes could have significant effect on the "brute force" technique to synchronize array elements. However this problem can be overcome in the ship application because the distances to the elements are known and will not change enough to significantly affect amplitude. In addition, the LNA gain in each module can be adjusted to compensate for differences in path length. Thus the synchronization technique should be tested on a full or smaller scale implementation of the WNODAR. This will allow relative tradeoffs in the choice of synchronization technique, hardware and software requirements to be fully analyzed and tested.

E. EFFECT OF DIGITAL PHASE SHIFTER QUANTIZATION

Digital phase shifter quantization introduces phase errors in the RF output signals and leads to pattern degradation. Consider the downconversion of the received signal. Let ω_s and ω_{LO} be the radian frequencies of the input signal and LO respectively. The input signal is

$$S(t) = \cos(\omega_s t) \tag{3.4}$$

Assume that the difference in path length $(r_{ref} - r_n)$ at element *n* is compensated by a four-bit digitization phase shift ϕ_n with a quantization error of Φ_n. Hence

$$k(r_{ref} - r_n) = \phi_n + \Phi_n \tag{3.5}$$

The LO signal at element *n* is

$$\begin{aligned} LO_n(t) &= \cos(\omega_{LO} t - k r_n - \phi_n) \\ &= \cos(\omega_{LO} t - k r_{ref} + \Phi_n) \end{aligned} \tag{3.6}$$

For direct conversion to baseband $\omega_{LO} = \omega_s$. After mixing and filtering, the output RF signal from element *n* is

$$RF_n(t) = \frac{1}{2}\cos(-k r_{ref} + \Phi_n) \tag{3.7}$$

Equation (3.7) shows that the RF signals from all elements are not exactly in phase from each other due to Φ_n. The phase quantization of the LO limits the phase coherence achievable by the array.

Reference [14] suggests that four-bit digitization is deemed satisfactory for digital phase shifter quantization for this application. The properties of primary concern are the gain and pointing direction of the main beam, and the sidelobe level. A more detailed analysis of the WNODAR's tolerance to phase errors is presented in Chapter IV. This section simply applies the respective formulas to assess the impact of phase errors Φ_n introduced by a four-bit synchronization phase shifter.

1. Reduction in Gain

Assuming the phase error of each element is uniformly distributed over the quantization interval, the fractional loss in gain is given by [17]

$$\frac{G}{G_0} = \left[\frac{\sin\left(\pi/2^m\right)}{\pi/2^m} \right]^2 \tag{3.8}$$

where

G_0 is the error free gain without quantization of phase

m number of bits used by the digital phase shifter.

Hence, a three-bit phase shifter causes a reduction in gain of 0.22 dB and a four-bit phase shifter has a gain reduction of 0.06 dB. Using the relationship derived between average transmit power and maximum detection range in the system tradeoff studies [10], the effect of a four-bit phase shifter is shown in Figure 22. For a 10 m^2 target, the theoretical maximum detection range of 2000 km is reduced by 12 km to 1988 km at the same average power of 500 W. Alternatively, a small 2.8% increase in average power from 500 W to 514 W will achieve the same detection range of 2000 km.

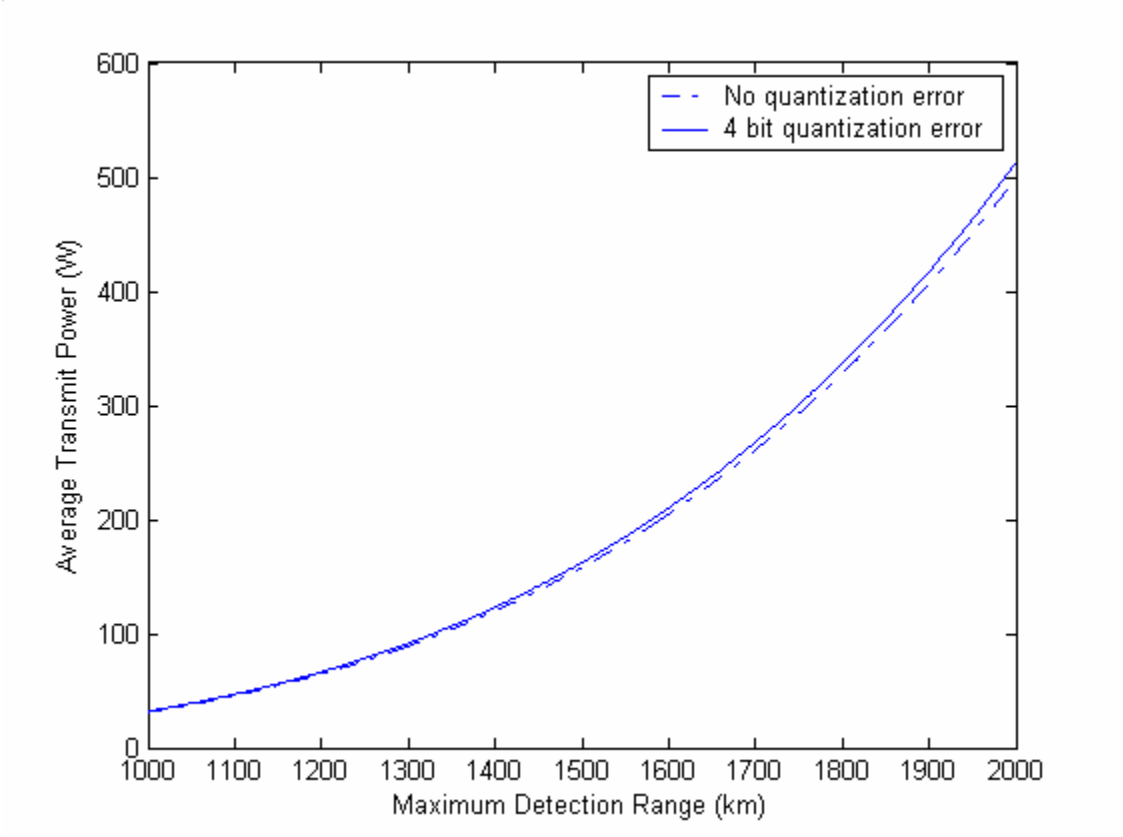

Figure 22. Relationship between average transmit power and maximum detection range.

2. Beam Pointing Error

If the phase error is evenly distributed, the mean pointing error is zero because the phase errors offset each other (zero mean). The RMS pointing error in radians is given by [17]

$$\sigma_u = \left(\frac{3}{N}\right)^{1/2} \frac{\Delta u \sigma_\Phi}{\pi} \tag{3.9}$$

where

N is the number of active elements

Δu is the beamwidth

σ_Φ is the RMS phase error.

Using results from the system tradeoff studies ($\Delta u = 5.41\times10^{-3}$ rad and $N = 787$) and a four-bit digitization ($\sigma_\Phi = 0.126$ rad), the calculated RMS pointing error is 1.34×10^{-5} rad or less than $0.001°$. The fractional pointing error is $\frac{\sigma_u}{\Delta u} = 2.48\times10^{-3}$, better than the generally satisfactory tolerance of 0.1.

3. Increase in Sidelobes

The sidelobe level at any given angle is the sum of the value at that angle due to the error free pattern plus a random quantity due to the phase errors. For modest phase errors ($\sigma_\Phi < 0.5$ rad), the mean increase relative to the main lobe is [17]

$$\frac{\sigma_\Phi^2}{N} \tag{3.10}$$

Results of the system tradeoff studies show that the average sidelobe gain relative to the mainlobe is $10\log_{10}\left(\frac{1}{N}\right) = -29.0$ dB. If four-bit digitization is used, a mean sidelobe increase of 0.1 dB is expected, resulting in an average sidelobe gain of -28.9 dB with respect to the main lobe. This is insignificant compared to the error free pattern.

Thus, we conclude that phase quantization by a four-bit synchronization phase shifter does not degrade the performance of the radar and is deemed sufficient for our application.

F. SUMMARY

Two techniques to perform element synchronization for the WNODAR were proposed. The “brute force” synchronization technique is a simple technique that can be easily implemented with a synchronization circuit in each element and in the beamformer/controller. The “beam tagging” synchronization technique takes less time, but requires more hardware modifications. Since the synchronization time is on the order of 2 to 3 μs, the more simple “brute force” technique is preferred. The problem faced by the “brute force” synchronization technique due to varying signal amplitudes can be

overcome in the ship application because the distances to the elements are known and will not change enough to significantly affect amplitude. In addition, the LNA gain in each module can be adjusted to compensate for differences in path length. The synchronization techniques should be tested on a full or smaller scale implementation of the WNODAR, allowing relative tradeoffs in the choice of synchronization technique, hardware and software requirements to be fully analyzed and tested. Finally it was concluded that a four-bit synchronization phase shifter does not degrade the performance of the radar. The phase error is expected to introduce a gain reduction of 0.06 dB. For a 10 m^2 target, the theoretical maximum detection range of 2000 km is reduced to 1988 km at an average power of 500 W. Alternatively, a small 2.8% increase in average power will achieve the same detection range of 2000 km. The expected RMS pointing error of less than $0.001°$ and a mean sidelobe increase of $0.1\,\mathrm{dB}$ with respect to the main lobe is insignificant compared to the error free pattern.

THIS PAGE INTENTIONALLY LEFT BLANK

IV. ELEMENT GEOLOCATION FOR THE WNODAR

Chapter III discussed techniques to synchronize array elements without explicit measurement of the elements' position. However, geolocation or knowledge of the elements' position is crucial in digital beamforming. In an opportunistic array, the individual elements are placed in open, available areas and the positions are continuously changing because the ship's superstructure is a dynamic platform. This fact must be taken into account in the signal processing to avoid degradation in the sidelobes, gain and beam pointing. In this chapter the effect of position errors is explained and a technical survey performed on applicable position location techniques methods. Their feasibility is examined based on performance and suitability for implementation. Finally, the effect of hull deflection on radar performance was simulated to determine the need for accurate and dynamic position sensing.

A. POSITION LOCATION UNCERTAINTY

1. Model

Consider an array of *N* elements spread throughout a volume, of which element *n* is shown in Figure 23. Let the position of element *n* be (x_n, y_n, z_n) and $\vec{r}_n$ is its position vector. The path length difference to the observation point between element *n* and the "reference element" at the origin is *R*. Assume all elements are isotropic radiators and neglect the mutual coupling and blockage between the elements. The normalized far-field array factor is

$$\begin{aligned} AF(\theta,\phi) &= \frac{1}{N}\sum_{n=1}^{N} A_n e^{j\left[\vec{k}\bullet\vec{r}_n\right]} \\ &= \frac{1}{N}\sum_{n=1}^{N} \left|A_n\right| e^{j\left[k\left(ux_n+vy_n+wz_n\right)+\Phi_n\right]} \end{aligned} \tag{4.1}$$

where

$k = \frac{2\pi}{\lambda}$ is the wave number

$\vec{k} = k\left(u\hat{x} + v\hat{y} + w\hat{z}\right)$

$u = \sin\theta\cos\phi$

$v = \sin\theta\sin\phi$

$w = \cos\theta$

$A_n = \left|A_n\right| e^{j\Phi_n}$ is the complex weighting factor for element *n*

Φ_n is the phase shift of element *n* relative to a "reference element" located at the origin. It is the sum of phase corrections from synchronization circuit, compensation for hardware and position errors, and phase to scan the beam.

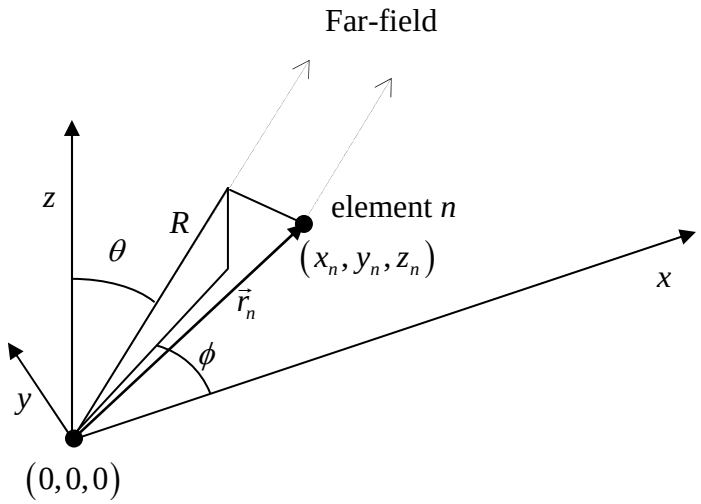

Figure 23. Geometry of elements in a volume.

Figure 24 shows the DD(X) WNODAR model and the coordinate system used. It is a CAD model of a DD(X) with 1200 randomly distributed elements. Depending on the scan direction of the main beam, not all elements contribute to the overall radiation pattern. Only those elements on surfaces whose normals $\hat{n}_n$ that are within ±90° of the scan direction contribute to the array factor. Elements that do not contribute are turned off. Hence, the element factor is defined as

$$EF_n = \begin{cases} 1, & \hat{k} \bullet \hat{n}_n > 0 \\ 0, & \text{otherwise} \end{cases} \tag{4.2}$$

The pattern factor is the product of the array factor and the element factor before the summation operation.

$$F(\theta,\phi) = \frac{1}{N}\sum_{n=1}^{N} |A_n| e^{j\left[\vec{k}\bullet\vec{r}_n + \Phi_n\right]} EF_n \tag{4.3}$$

Typical plots of the pattern factor generated using Equation (4.3) are shown in Figure 25. It is assumed that there are no excitation errors and all elements are equally weighted, $|A_n| = 1$. Figure 25(a) shows a broadside scan $(\phi_s = 90°)$ at an elevation of $10° \left(\theta_s = 80°\right)$ and Figure 25(b) shows an endfire scan $(\phi_s = 180°)$ in the forward direction, at the same elevation. The broadside scan produces a narrower beamwidth than the endfire scan because at broadside the elements that contribute to the pattern factor are spread over a much longer distance, corresponding to a larger effective aperture.

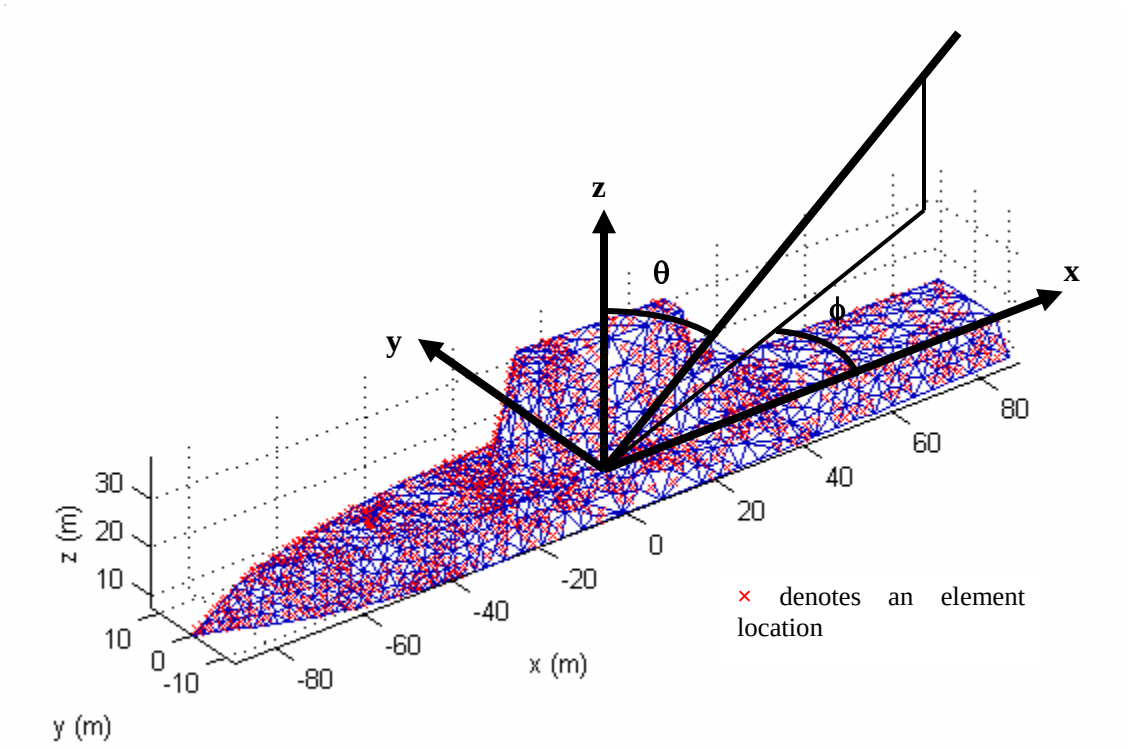

Figure 24. DD(X) model with 1200 randomly distributed elements.

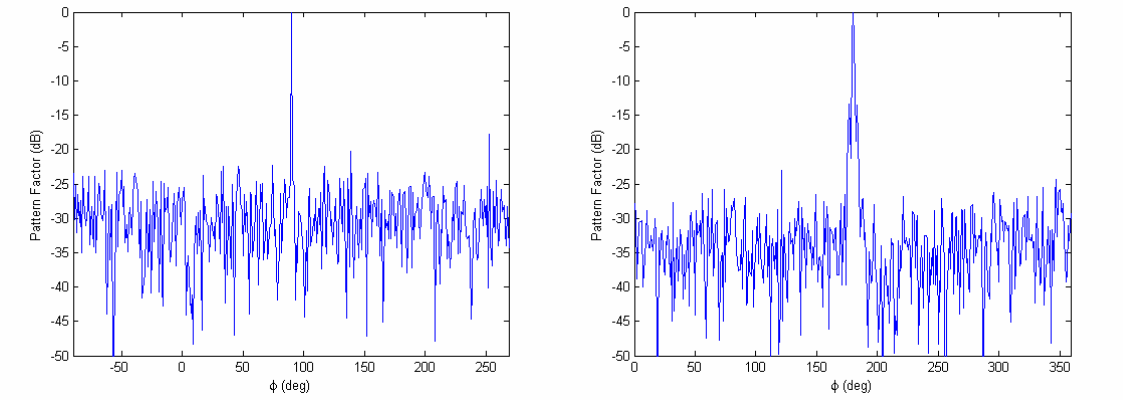

(a) (b)

Figure 25. Sample pattern factors for 1200 element array.
(a) Broadside scan $(\phi_s = 90°)$ (b) Endfire scan $(\phi_s = 180°)$.

2. Tolerance Theory

Let $F_0(\theta,\phi)$ be the error free pattern factor. Assume there are no excitation errors and all elements are equally weighted, $|A_n|=1$. If element *n* is displaced from the design coordinates by position errors Δx_n, Δy_n and Δz_n, the pattern factor is

$$F(\theta,\phi)=\frac{1}{N}\sum_{n=1}^{N} e^{j\left[\vec{k}\bullet\vec{r}_n+\Phi_n\right]} e^{j\delta\Phi_n} EF_n \tag{4.4}$$

where the phase shift (path length difference) introduced in element *n* is

$$\delta\Phi_n = k\left(u\Delta x_n + v\Delta y_n + w\Delta z_n\right) \tag{4.5}$$

Hence, the location errors affect the phases of the signals across the array. The power pattern is the product of Equation (4.4) and its complex conjugate. Its expected value is

$$E\left(FF^*\right)=\frac{1}{N^2}E\left(\sum_{n=1}^{N}\sum_{m=1}^{N} e^{j\left[\vec{k}\bullet\vec{r}_n-\vec{k}\bullet\vec{r}_m+\Phi_n-\Phi_m\right]} e^{j(\delta\Phi_n-\delta\Phi_m)} EF^2\right) \tag{4.6}$$

Equation (4.6) can be simplified assuming the means of the phase errors are zero and all errors are independent of each other. We can also drop the element factor by replacing N with N', the number of active elements. The expected value becomes [17]

$$E\left(FF^*\right)=\left|\overline{e^{j\delta\Phi}}\right|^2\left|F_0\right|^2+\frac{1-\left|\overline{e^{j\delta\Phi}}\right|^2}{N'} \tag{4.7}$$

The first term is the error free pattern $|F_0|^2$, reduced by a factor which depends on the phase errors. The second term represents a statistical average side-lobe level, an angle-independent contribution to the expected power pattern, where its magnitude is inversely proportional to the number of active elements. Since the normalized error free, main beam gain is $\left|F_0(\theta_s,\phi_s)\right|^2=1$, the main beam gain relative to the error free main beam gain is

$$\frac{G}{G_0}=\left|\overline{e^{j\delta\Phi}}\right|^2+\frac{1-\left|\overline{e^{j\delta\Phi}}\right|^2}{N'} \tag{4.8}$$

The limiting value of the loss as the number of elements grows is

$$\frac{G}{G_0} = \left|\overline{e^{j\sigma_\Phi}}\right|^2 = \left|\int e^{j\sigma_\Phi} w(\sigma_\Phi)\, d\sigma_\Phi\right|^2 \tag{4.9}$$

where $w(\sigma_\Phi)$ is the pdf of the phase error σ_Φ.

3. Reduction in Gain

Equation (3.8) that was used earlier can be derived by evaluating Equation (4.9) for a uniform distribution $w(\sigma_\Phi)$. If the phase error is a normal distribution where σ_Φ^2 is the variance of the phase shift error across the array, the loss in the main lobe gain is [17]

$$\frac{G}{G_o} = e^{-\sigma_\Phi^2} \tag{4.10}$$

The tolerance is arbitrarily taken to be $\sigma_\Phi = 0.5$ rad, which limits the loss in gain to 1 dB. The tolerance on the phase shift error determines the tolerance on the position errors. The RMS phase variation is equivalent to a RMS position error of 0.0796λ, hence the general rule of thumb that errors in position of the elements on the order of 0.1λ may be tolerated [18].

Preliminary radar system studies [6] have selected the upper VHF or lower UHF frequency operating band for the WNODAR. Assuming an operating frequency of 300 MHz, the position location system must be able to locate the elements with a position accuracy of 10 cm. Using the results from the system tradeoff studies, a position error of 10 cm that results in a 1 dB loss in gain reduces the theoretical maximum detection range from 2000 km to 1785 km. Alternatively, an increase in average power from 500 W to 791 W will achieve the same detection range of 2000 km.

4. Beam Pointing Error

The RMS pointing error in radians is the same as before

$$\sigma_u = \left(\frac{3}{N'}\right)^{1/2} \frac{\Delta u \sigma_\Phi}{\pi} \tag{4.11}$$

Using results from the system tradeoff studies ($\Delta u = 5.41\times10^{-3}$ rad and $N = 787$) and tolerance phase error of $\sigma_\Phi = 0.5$ rad, the calculated RMS pointing error is 5.32×10^{-5} rad or $0.003°$. The fractional pointing error is $\frac{\sigma_u}{\Delta u} = 9.83\times10^{-3}$, better than the generally satisfactory tolerance of 0.1.

5. Increase in Sidelobes

The expected increase in sidelobe level relative to the main lobe is

$$\frac{\sigma_\Phi^2}{N'} \tag{4.12}$$

Using the tolerance phase error of $\sigma_\Phi = 0.5$ rad, the mean sidelobe increase of 1.0 dB is expected, resulting in an average sidelobe gain of -28.0 dB with respect to the mainlobe. This increase is insignificant.

Hence, as long as the tolerance phase error of $\sigma_\Phi = 0.5$ rad is met, the radar's performance in terms of gain, beam pointing and sidelobe levels is not significantly affected.

B. SURVEY OF POSITION LOCATION TECHNIQUES

Position location of elements is commonly achieved by lateration, which is to measure an object's distance from multiple reference positions. In a wireless environment, networked transceivers can obtain distance measurements by one or combination of the following ways:

1. Transmit a signal of known velocity from the reference position to the object, measure the time of flight (TOF) to calculate distance. This requires all receivers and transmitters to be perfectly synchronized.

2. If receivers and transmitters are not synchronized, transmit two or more signals simultaneously and program the receivers to measure the time difference of arrival (TDOA) to calculate distance.

3. Use angles to calculate distance. Angle of arrival (AOA) technique requires accurate angle information, typically using phased antenna arrays with multiple antennas and known separation to perform angular calculation.

4. Derive a function correlating attenuation and distance for a transmitted signal. Estimate distance by measuring the received signal strength (RSS) when a reference signal reaches the object.

There is a wide variety of commercially available position location systems for navigation, communication, and asset tracking applications. They generally apply one or combination of TOF, TDOA, AOA and RSS to measure an object's distance from three or more reference points. They also operate at various frequencies, employ a variety of signal waveforms and incorporate signal processing to improve performance. Because of this, performances of position location systems vary in accuracy, coverage and cost of implementation.

For the WNODAR, the position location technique should be able to locate array elements under the following circumstances:

1. Provide centimeter level accuracy. This is 10% of the position error tolerance of 0.1λ, and is deemed sufficient for accurate digital beamforming.

2. Perform in a severe multipath environment. Array elements are placed in open, available areas, subject to blockages from stationary structure and moving equipment. The location system must operate over the area of the ship and maintain accuracy under dynamic non line-of-sight (non-LOS) conditions.

3. Satisfy other factors including reasonable system and infrastructure cost, ease of implementation and compatibility with characteristics of the opportunistic array concept.

The following section evaluates several candidate commercial position location techniques for suitability of implementation in the opportunistic array.

1. Global Positioning System (GPS) Based Systems

The GPS is one the most widely used location-sensing systems. GPS provides an excellent lateration framework for determining geographic positions. GPS satellites are precisely synchronized with each other and transmit their local time in the signal allowing receiver to compute the difference in TOF. Its worldwide satellite constellation has reliable and ubiquitous coverage. The standard GPS receiver used with a differential reference or use of the Wide Area Augmentation System, can compute location to less than 3 m on average [19]. However, GPS based systems have limitations. GPS receivers need an antenna of sufficient size for adequate satellite reception, they only work well with a relatively unobstructed and geometrically good satellite constellation, and they suffer from relatively slow update rates (1 Hz for Garmin GPS V).

Joint Precision Approach and Landing System (JPALS). The sea based JPALS works with GPS to provide accurate and uninterrupted landing guidance for fixed and rotary-wing aircraft during category I and II visibility conditions. JPALS uses a relative carrier phase based differential technique (using a base station) to provide a lateral and vertical accuracy of 0.3 m over an area of 30 nm radius [20]. Differential operation is used to reduce orbit errors, spatially correlated errors due to the atmosphere, and eliminate both receiver and satellite clock biases. The main disadvantage for JPALS like all GPS based systems, is that LOS transmission to the base station is required for reliable operation.

Pseudolite Transceivers. In situations where GPS satellite geometry is poor or the signal availability is limited, ground based transmitters of GPS-like signals (called “pseudolites”) can be used to augment GPS. This requires infrastructure of at least four reference beacons to be set up to replace the satellite constellation. Carrier phase observation is usually employed to determine a three-dimensional position from reference beacons. A prototype pseudolite system developed by Locata Corporation performed static carrier phase point positioning with subcentimeter precision over an area of 200 m × 60 m [21]. The system requires four LocataLites (time-synchronized pseudolite transceivers) to perform carrier point positioning (CPP) to determine its three-dimensional position.

GPS based systems are not suitable for our application. The key disadvantage is the need to for LOS between the sensors and the measuring units. As shown in Figure 26, the multiple measuring units will have to be located on the ship's surface in view of element. This limits the possible deployment locations for the sensor elements and does not maximize the wireless opportunistic array concept. Even if this is tolerable, LOS will still be affected by moving structures and equipment, personnel movement and environmental conditions (smoke, fog, etc.).

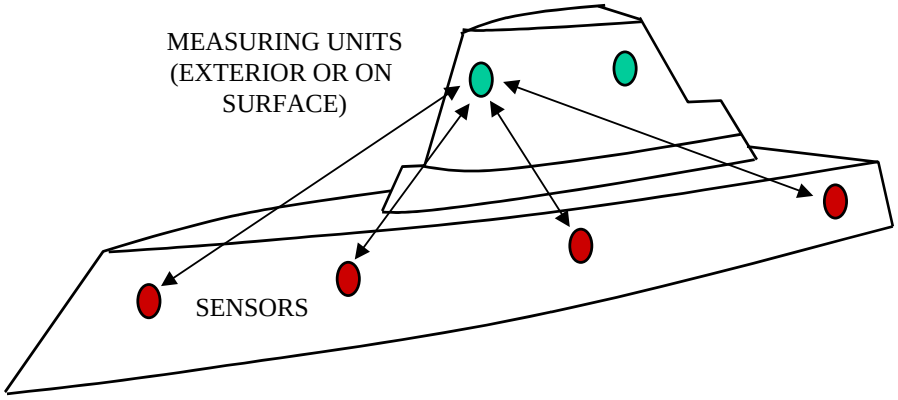

Figure 26. Measuring units placed in unobstructed view of sensors.

2. Wireless Local Area Network (WLAN) Based Systems

The proliferation of mobile computing devices and wireless networks has fuelled a growing interest in location-aware systems and services. WLAN (IEEE 802.11b) radio-signal-based positioning system has distinct advantages for being commercially available, easily adaptable and having robust signal propagation. For example, a Microsoft Research group developed RADAR [22], a building-wide tracking system that measures at the base station, the received signal strength (RSS) and signal-to-noise ratio of signals that wireless devices send, then uses this data to compute the two-dimensional position. RADAR's scene-analysis implementation can place objects to within about 3 m of their actual position with 50% probability. Several commercial companies such as WhereNet and Pinpoint sell wireless asset-tracking packages, which are similar in form to RADAR. Pinpoint's 3D-iD performs indoor position tracking using proprietary base station and tag hardware to measure radio TOF. Pinpoint's system can achieve 1 to 3 m accuracy.

LOS is generally not required for WLAN based systems but the system needs to build a radio map of marked locations and the observed RSS and apply search algorithms to determine the best match for the signal strength samples measured at the base stations. In environments with many obstructions, such as onboard a ship, measuring distance using RSS and signal attenuation is usually less accurate than TOF. Signal propagation issues such as reflection, refraction and multipath cause attenuation to correlate poorly with distance.

3. Ultrasound Based Systems

Position sensing systems based on ultrasound devices take advantage of the TDOA between ultrasound and RF signals to measure distance. In the Cricket Location Support System, beacons transmit concurrent RF and ultrasound pulses. The listener obtains a distance estimate for the corresponding beacon by taking advantage of the difference in propagation speeds between RF (speed of light) and ultrasound (speed of sound). Although it can provide distance ranging and positioning precision of 1 to 3 cm [23], much initial configuration work is needed for beacon deployment. LOS for ultrasound based systems is required, and must be overcome by suitable placement of beacons.

4. Frequency Modulated Continuous Wave Systems

The Frequency Modulated Continuous Wave (FMCW) radar uses modulated high frequencies (typically microwave frequencies) so that the frequency difference between the reflected and the transmitted signal is proportional to the distance to the object ahead. It is common in vehicle collision avoidance sensors with advantages of being insensitive to mud and poor visibility conditions. FMCW is also widely used for industrial sensors due to its high sensitivity and good reliability. ELVA-1's 94 GHz Millimeter Wave Industrial Distance Sensor provides excellent penetration of dust and water vapor, because of its 3 mm wavelength. The operation range of the distance sensor is 300 m with accuracy of 1 cm [24].

5. Ultra-Wideband Based Systems

A proven technique for position location under non-LOS operations is the use of ultra-wideband systems. The Office of Naval Research (ONR) Naval Total Asset Visibility (NTAV) program investigated several asset visibility technologies for shipboard application and selected ultra-wideband (UWB) technology because of its improved ability to operate in high multipath environments and increased accuracy over conventional systems [25]. UWB technology's very wide bandwidth property offers the advantage that its lower frequencies penetrate walls and the ground enabling indoor localization applications. UWB technology also offers low system complexity and low cost. UWB systems can be made nearly "all-digital," with minimal RF or microwave electronics. Because of the inherent RF simplicity of UWB designs, these systems are highly frequency adaptive, enabling them to be positioned anywhere within the RF spectrum. This feature avoids interference to existing services, while fully utilizing the available spectrum.

The PAL650 (Precision Asset Location 650) UWB system has indoor range of 300 feet and accuracy of 1 foot at operating frequency 6.2 GHz. A recent release of the new Sapphire product line provides precision localization to 10 cm resolution. UWB systems similar to the PAL650 have been successfully tested in a shipboard environment, where radio transmissions proved to be especially difficult because the ships metal superstructure feature many reflections. UWB signals were shown to propagate well aboard ships, into corners, through cracks between containers, and around objects so that reasonably accurate positions can be determined.

6. Summary of Survey

A survey of current state-of-art location sensing methods was conducted. The problem of position determination for elements in a wireless opportunistic array can be tackled through commercial solutions for geolocation. Under relatively benign propagation conditions, most systems are producing centimeter level accuracy, which is a fraction of the array's operating wavelength of about 1 m, and within the tolerable limit of 0.1λ position error. For elements placed in a high multipath environment like the

ship's open deck, UWB systems appear to be the technology of choice because of its ability to perform in the presence of objects obstructing LOS, as well as its simplicity and flexibility in design.

C. SHIP HULL DEFLECTION

Studies have shown that stresses on a ship's hull are generally most severe in the vertical bending mode, known as hogging and sagging. This is mainly caused by unequal distributions of weight and buoyancy along the length of the ship, accentuated by the variation of buoyancy forces due to the passage of waves. The ship can also bend in the horizontal plane or twist due to unequal sideways forces from waves, although these types of distortions are generally less significant.

Previous research was conducted to analyze the effect of commonly occurring ship load variations and wave induced bending moments on hull girder flexure for the FFG7 class of U.S. Navy frigates [26]. The Ship Hull Characteristics Program (SHCP), the U.S. Navy's standard hydrostatics program was used to compute the hull deflection from the full load condition in seastates 0, 4, and 6, shown in Figure 27. The deflections for seastate 2 are not included because they are not appreciably different from the deflection at still water. The deflections are due to wave action and are dynamic with respect to the seastate 0 deflection. The maximum hull deflection is 0.14 m at seastate 4 and 0.20 m at seastate 6.

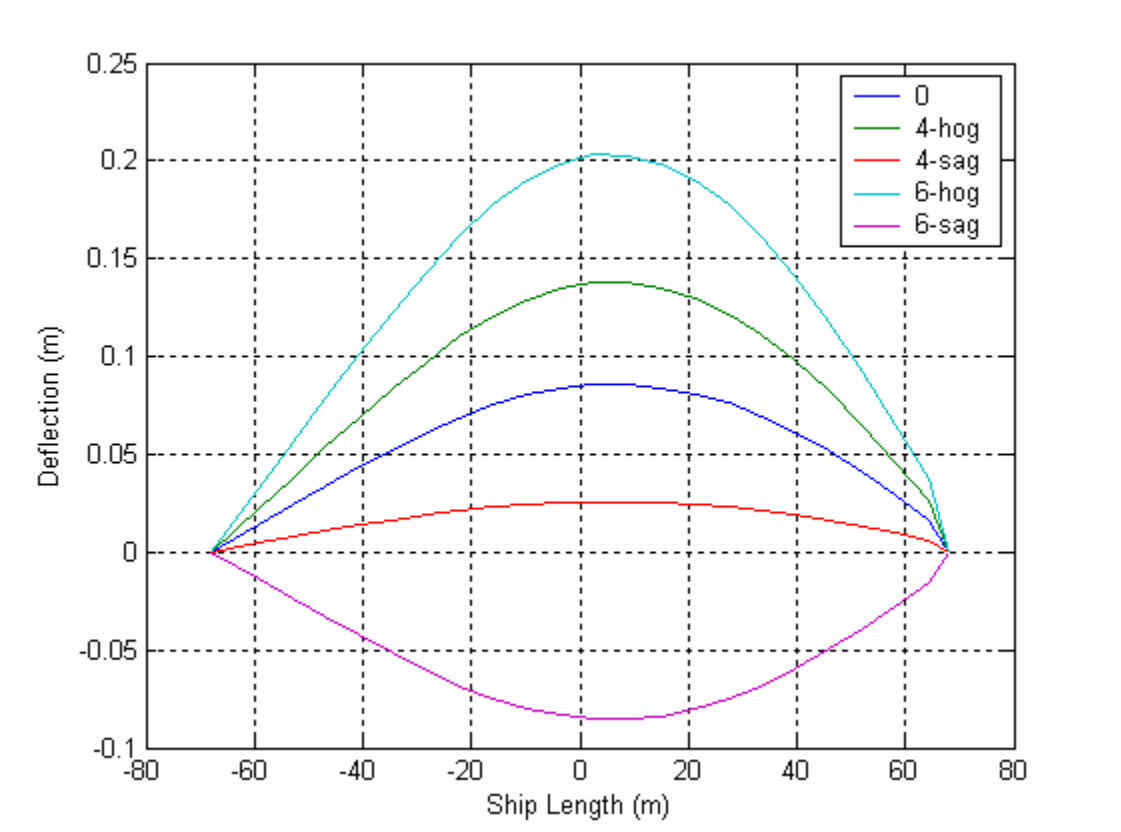

Figure 27. Hull deflection of FFG7 under full load and different seastate conditions.

Since the hull deflection data for the DD(X) ship (length 600 ft) is not available, the data for the FFG7 (length = 445 ft) is scaled by a proportional factor to extrapolate the equivalent hull deflection data. Figure 28 shows a broadside profile of the sensor elements. Since the ship hull deflection is primarily in the vertical bending mode, the position error is mainly in the z coordinates. The right *y*-axis shows the estimated position error, Δz at various points along the ship's length under different seastate conditions. This data will be used to investigate the effect of ship hull deflection on the performance of the WNODAR to be discussed next.

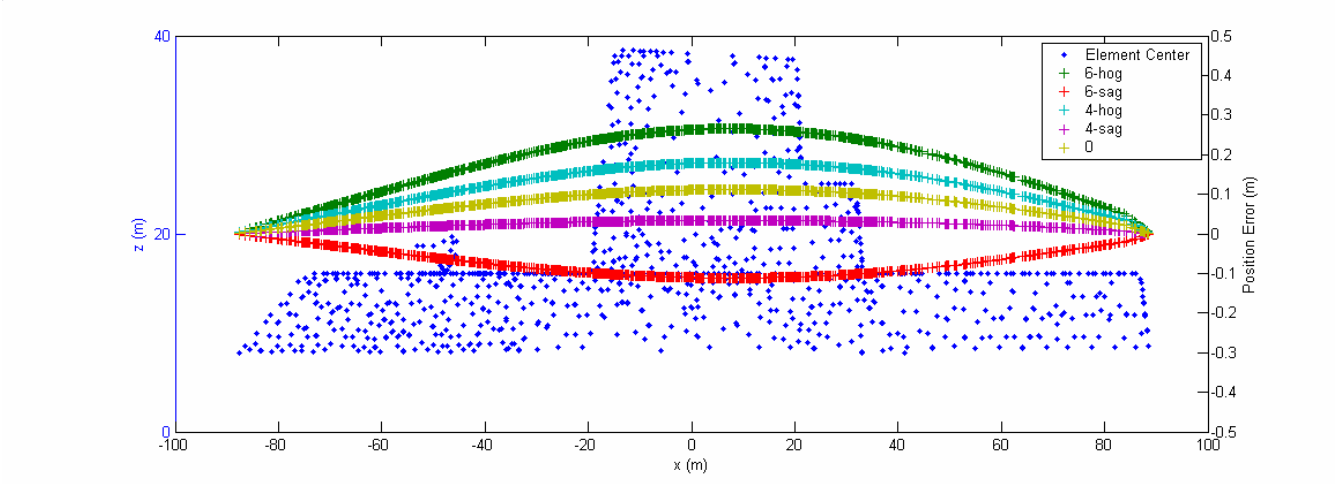

Figure 28. Estimated hull deflection of DD(X) under different seastate conditions.

D. SIMULATION

Simulation consists of two parts. In the first part, the predicted effects of phase errors are compared with the simulated pattern factor generated by the DD(X) WNODAR model. In the second part, the hull deflection data from Section C is used to generate the phase errors likely to be encountered on a DD(X). This allows the performance of the radar to be evaluated under more realistic conditions.

Table 3 summarizes the effect of digitization and position errors on pattern factor gain and sidelobe levels. The simulation is for a broadside scan $(\phi_s = 90°)$ at an elevation of $10°$ $(\theta_s = 80°)$. Simulated results are close to theory predictions. Using four-bit digitization and assuming 10 cm dynamic position error, a gain reduction of -0.63 dB and an increased average sidelobe level of -29.0 dB is expected. The gain reduction reduces the theoretical maximum detection range from 2000 km to 1863 km. An increase in average power from 500 W to 667 W is required to compensate for the reduction in gain. The position error of 0.1λ gives better gain performance than the tolerance of $\sigma_\Phi = 0.5$ rad. This is because in a three-dimensional array, the position error is equally distributed in the *x*, *y* and *z* coordinates, the equivalent RMS position error in

each axis is $0.0577\lambda = 0.36$ rad. The gain reduction is the more significant degradation compared to increase in average sidelobe level. Hence the effect of gain reduction is studied in greater detail in the next part of simulation.

	Theory		**Simulation**	
	Four-bit digitization error	$\sigma_\Phi = 0.5$ rad **position error**	**Error free pattern**	**Four-bit digitization and** 0.1λ **position error**
Gain reduction relative to error free pattern	–0.06 dB	–1 dB	0 dB	–0.63 dB
Maximum detection range	1988 km	1785 km	2000 km	1863 km
Average power required to compensate loss in gain (% increase)	514 W (2.8%)	791 W (58%)	500 W (0%)	667 W (33%)
Sidelobe level with respect to mainlobe	–28.9 dB	–28.0 dB	–29.5 dB	–29.0 dB

Table 3. Effect of digitization and position errors on pattern factor gain and sidelobe levels.

In the second part of this simulation, hull deflection data from Section C is used to generate the phase errors likely to be encountered on a DD(X). This allows the performance of the radar to be evaluated under more realistic conditions. Figure 29 shows that the gain reduction is between –0.056 dB under seastate 4-sag conditions, to the worst case of –0.070 dB under seastate 6-hog conditions. The reason why the gain reduction is little, even for position errors greater than 20 cm (0.2λ) can be understood by observing Equation (4.5), which is repeated here:

$$\delta\Phi_n = k\left(\sin\theta\cos\phi\,\Delta x_n + \sin\theta\sin\phi\,\Delta y_n + \cos\theta\,\Delta z_n\right) \tag{4.13}$$

Hull deflection contributes mainly to height errors, Δz_n. But for a broadside scan at an elevation of 10° $(\theta = 80°)$, the contribution to phase error is low because of the cosine factor. The stronger dependence of pattern gain on scan elevation, is demonstrated in

Figure 30. At elevation of $30°\,(\theta = 60°)$, a gain reduction of more than $-0.25\,\text{dB}$ is expected. But for BMD applications, long range targets are expected near the horizon, at elevation of 0 to $10°$. Hence the effect of gain reduction with increasing elevation angles is not an issue of concern.

Finally, a set of performance curves for the WNODAR is obtained. Figure 31 shows data for the WNODAR operating under dynamic conditions, taking into account the effects of hull deflection under different seastate conditions, and the use of four-bit synchronization phase shifters. For an average transmission power of 500 W, a maximum detection range of 1990 km for a 10 m^2 target is obtained under seastate 6 conditions. This is only a reduction of 0.5% from the error free condition. Alternatively, a 2% increase in average transmission power is required to maintain a maximum detection range of 2000 km under the same conditions.

Hence, at this time, analysis and simulation results suggest that a position location scheme to correct for dynamic effects of hull deflection is not absolutely necessary for an array operating at a VHF or lower UHF frequency. The additional cost and complexity of the position location system would not significantly improve the radar's performance.

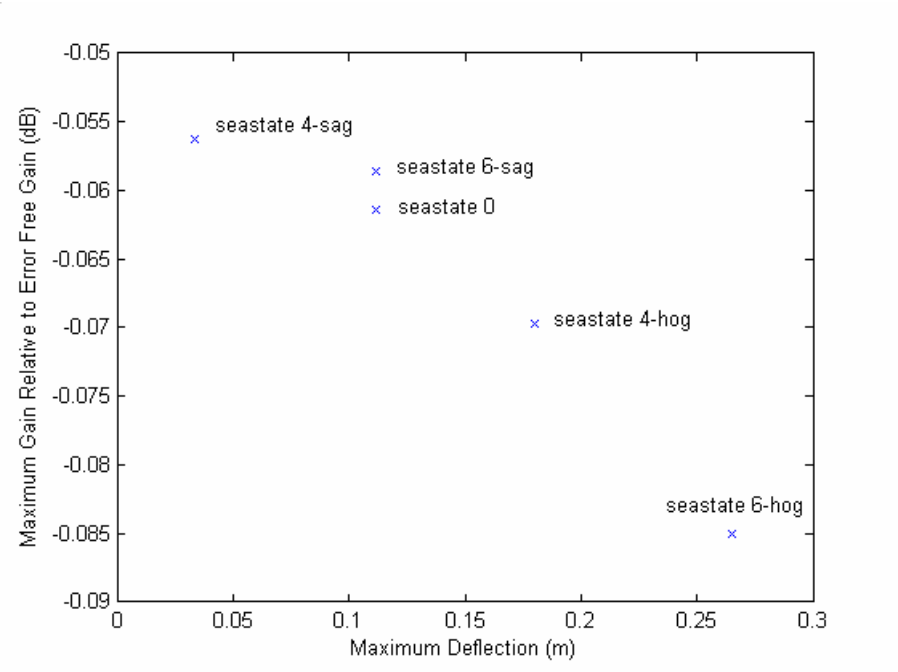

Figure 29. Maximum gain relative to error free gain under different seastate conditions.

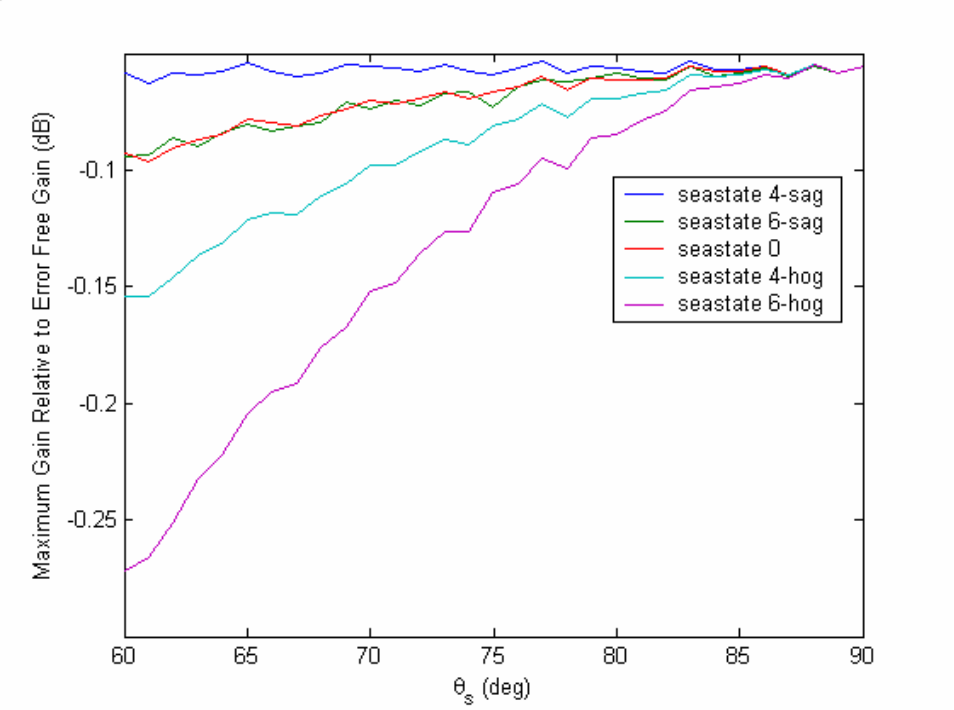

Figure 30. Relationship between maximum gain and scan angle θ_s.

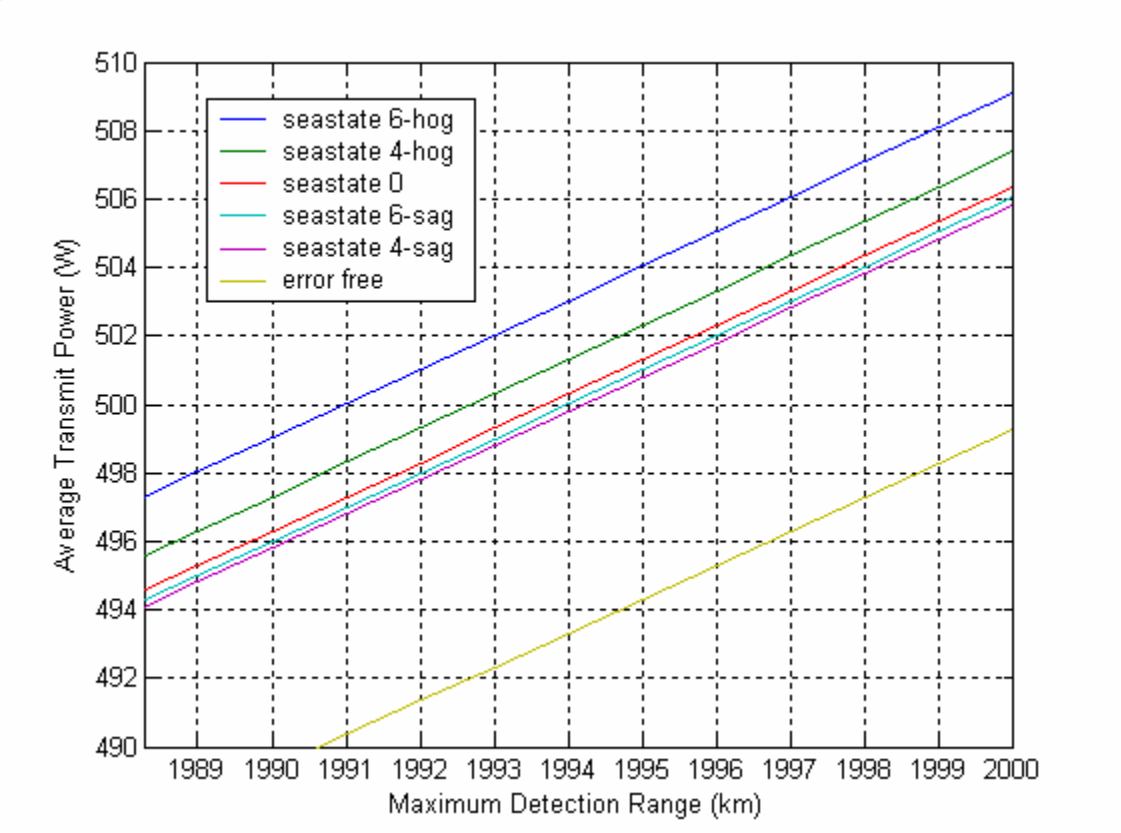

Figure 31. Performance curves for the WNODAR under different seastate conditions.

E. SUMMARY

This chapter has shown that the problem of position determination for elements in a WNODAR can be tackled through commercial solutions for geolocation. Under relatively benign propagation conditions, most systems are producing centimeter level accuracy, which is a fraction of the array's operating wavelength of about 1 m and within the tolerable limit of 0.1λ position error. Using conventional hull deflection data and extrapolating to the DD(X), a set of performance curves for the WNODAR was obtained. The curves show the performance of the WNODAR operating under dynamic conditions, taking into account the effects of hull deflection under different seastate conditions, and the use of four-bit synchronization phase shifters. For a nominal average transmission power of 500 W, a maximum detection range of 1990 km for a 10 m^2 target is obtained under seastate 6 conditions. This is only a reduction of 0.5% from the error free condition. Alternatively, a 2% increase in average transmission power is required to maintain a maximum detection range of 2000 km under the same conditions. Hence, at this time, analysis and simulation results suggest that a position location scheme to correct for dynamic effects of hull deflection is not absolutely necessary for an array operating at a VHF or lower UHF frequency.

THIS PAGE INTENTIONALLY LEFT BLANK

V. DESIGN OF A DEMONSTRATION T/R MODULE

The next phase of research is the development of a demonstration T/R module to validate the wireless opportunistic array concept. The design of the demonstration T/R module takes advantage of advance technology adopted from commercial markets such as cellular telephony. Two main thrusts are identified. Firstly the use of field programmable gate array (FPGA) for digital radar implementation. And secondly, the use of high data rate wireless communications for the wireless link. Following the outline of these technologies, this chapter presents the proposed architecture and candidate hardware for a demonstration T/R module. Taking a step further, the projected communication requirements for the full-scale WNODAR are matched against current technology. The solution to gigabit data transmission rates using commercially available wireless communication systems is discussed.

A. FPGA AND WIRELESS COMMUNICATION TECHNOLOGIES

1. FPGA Devices

One of the key performance advantages of the WNODAR is its digital architecture. Digital radar processing functions such as digital beamforming are particularly demanding and are usually built with custom application specific integrated circuits. But the advances in the speed and size of FPGAs have allowed many high end signal processing applications to be solved in commercially available hardware. A FPGA is a device that contains a matrix of configurable gate array logic circuitry that is programmed with software. When a FPGA is configured, the internal circuitry is connected in a way that creates a hardware implementation of the hardware application. Thus FPGA devices deliver the performance reliability of dedicated hardware circuitry.

FPGAs are well suited for very high-speed parallel multiply and accumulate functions. Current generation FPGAs can perform an 18 bit $\times$ 18 bit multiplication operation at speeds in excess of 200 MHz. This makes FPGAs an ideal platform for operations such as Fast Fourier Transform (FFT), Finite Impulse Response (FIR) filters,

digital down/up converters, correlators and pulse compression operators, which are the fundamental processes for radar processing [27]. FPGAs have been implemented in phased array radar beamformers, in smart antennas for wireless base stations and in real-time high-bandwidth spectrum monitoring.

For the development of a demonstration T/R module, FPGA-based hardware provides the ability to define custom measurement and control hardware quickly and economically. Hence, its high performance, flexibility and commercial availability are key advantages over the use of conventional application specific hardware.

2. High Data Rate Wireless Communication Systems

The wireless opportunistic array concept demands very high data rate wireless communication. Hundreds or even thousands of self-standing T/R modules continuously communicate element localization and synchronization signals, beam control data, and digitized radar signals wirelessly with the central signal processor. Fortunately, wireless communication has received significant attention in recent years. This has led to a wide variety of low-cost, high performance, wireless communication systems that help make digital antenna a cost effective option.

Currently, wireless local area networks (WLANs) offer peak rates of 10 Mb/s, with 50 Mb/s to 100 Mb/s becoming available soon. But there is still impetus to improve, given the demand for higher access speeds due to the increase in rich media content and competition from 10 Gb/s wired LANs. Additionally, future home audio/visual A/V networks will be required to support multiple high-speed high-definition television (HDTV) A/V streams, which demand near 1 Gb/s data rates. Besides high data rate, another research focus is on operating in non-LOS environment, which induces random fluctuations in signal level, known as fading [28].

The design of the demonstration T/R module leverages on commercial wireless communication systems. For the demonstration T/R module, a sub-Gb/s wireless link is sufficient since only a limited number of T/R modules will be needed in the validation phase. However, the full scale system will demand a much higher data rate wireless link. In addition, elements in a WNODAR need to communicate in a non-LOS environment,

due to obstruction from ship structures. Hence current developments in wireless communication systems directly support the requirements for the WNODAR.

B. PROPOSED DEMONSTRATION T/R MODULE DESIGN

A block diagram of the demonstration T/R module is shown in Figure 32. The demonstration system is a scaled down version of the WNODAR, with only a handful of elements. Its main purpose is to prove the feasibility of the wireless T/R module concept. The carrier frequency of 2.4 GHz is used instead of the 300 MHz as recommended from the system tradeoff study. This is because of the wide selection of low cost commercial products operating in this frequency band. The digital transmitter and receiver is the core of the T/R module. It comprises the FPGA hardware and the modulator/demodulators. The wireless modem comprising RF modules and integrated circuits provide media access control over the wireless data link. It operates at frequencies different from the carrier to avoid interference. The key components of the T/R module design are presented in the following section.

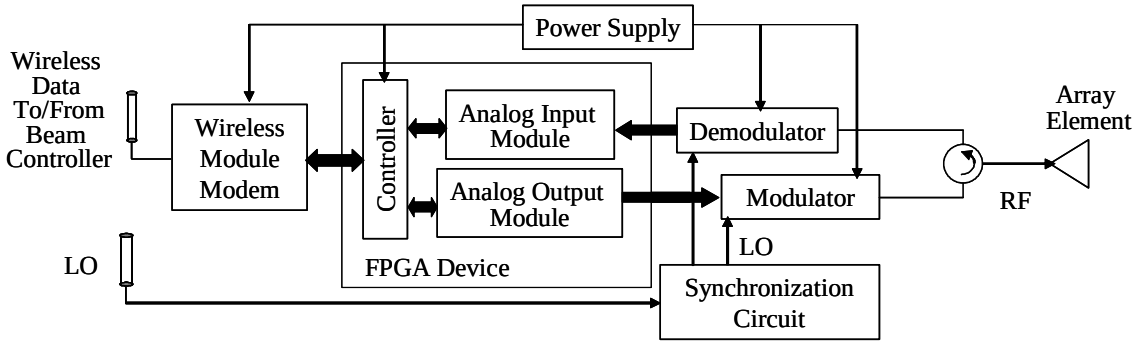

Figure 32. Block diagram of the proposed demonstration T/R module (From [13]).

1. Digital Transmitter and Receiver

The digital transmitter and receiver is implemented on FPGA hardware. It consists of a controller interfaced with A/D and D/A data acquisition modules. The controller receives wireless data from the beam controller, via the wireless module modem, to generate the transmit waveform. Wireless data from the beam controller includes control messages for setting timing, waveform parameters and phase synchronization commands. On receive, the controller sends the received radar signals

back to the beam controller for processing. The beam controller can be implemented real-time or offline on a PC. For offline operation, the outputs from the modem are stored for subsequent retrieval and processing.

The proposed FPGA hardware is the National Instruments (NI) CompactRIO reconfigurable embedded system as shown in Figure 33. It contains a real-time embedded processor and a four slot reconfigurable chassis containing a user programmable FPGA. It is used with the cRIO9215 analog input modules, which are able to sample analog inputs between ±10 V from four channels, with 16 bit quantization at 100 kS/s per channel, and the cRIO9263 analog output modules, able to ouput ±10 V from four channels, with 16 bit quantization at 100 kS/s per channel. The CompactRIO is programmable using the LabVIEW application, the FPGA circuitry is a parallel processing reconfigurable computing engine that executes the LabVIEW application in silicon circuitry on a chip. Another advantage of FPGA implementation is that radar transmit waveforms can be generated in the controller and this eliminates the need for a DDS.

Figure 33. National Instruments (NI) CompactRIO controller and I/O module (From [29]).

Two I/O modules are required to interface with the demodulator and modulator of a T/R module. Hence one CompactRIO controller with a four slot chassis can control a modulator and demodulator plus any switches that might be needed. The current cost of the demonstration T/R module is about $3,500 per element. The size of the demonstration system will be determined by available funds at the time of construction.

2. Modulator and Demodulator

The modulator and demodulator follow conventional radar design. The radar transmit waveform generated by the FPGA is directly up-converted to the operating band, power amplified and applied to the antenna via a circulator. On receive, the waveform is downconverted to baseband, and the baseband in-phase and quadrature signals are sent to the FPGA for further processing.

The AD8346EVAL modulator board on the transmit end and its complimentary AD8347EVAL demodulator board on the receive end are selected. The AD8347EVAL demodulator board is a broadband direct quadrature demodulator with RF and baseband Automatic Gain Control (AGC) amplifiers. It performs quadrature demodulation directly to baseband frequencies. The input frequency range of the board ranges from 0.8 to 2.7 GHz. The AD8347EVAL demodulator board, shown in Figure 34, directly down-converts the RF signal to *I* and *Q* baseband components after mixing with the LO signal. The *I* and *Q* voltage outputs are measured at four channels, the in-phase output positive (IOPP), in-phase output negative (IOPN), quadrature-phase output positive (QOPP) and quadrature-phase output negative (QOPN).

At the controller, the FPGA recovers the amplitude and phase of the received signal from the *I* and *Q* voltage outputs. The instantaneous voltages $I(t)$ and $Q(t)$ voltages are calculated by taking the differences (IOPP – IOPN) and (QOPP – QOPN) respectively. The amplitude $A(t)$ and phase $\Phi(t)$ of the received signal can be recovered using

$$A(t) = \sqrt{I(t)^2 + Q(t)^2} \tag{5.1}$$

$$\Phi(t) = \tan^{-1}\left[\frac{Q(t)}{I(t)}\right] \tag{5.2}$$

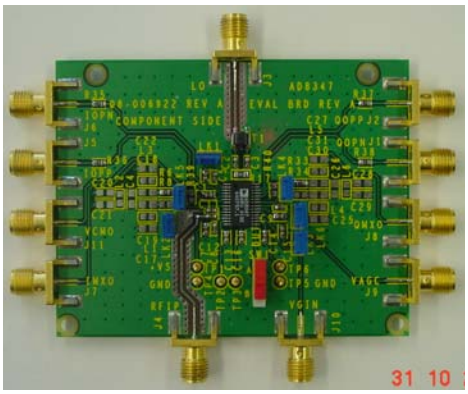

Figure 34. AD8347EVAL demodulator board.

3. LO Distribution and Synchronization

The LO reference signal must be distributed to the modulators and demodulators. Synchronization of the LO reference signal is necessary to lower the sidelobe levels and improve the pointing accuracy of the beam and also for any coherent processing of radar returns (i.e., coherent integration). The LO reference signal can be distributed wirelessly; a synchronization circuit is used to control phase corrections due to element dynamic position changes and propagation channel changes. Either the "brute force" or "beam tagging" algorithm can be used, as discussed in Chapter III.

In order to avoid the need for additional hardware (i.e., the synchronization circuit) and to exploit the additional computation capability of the FPGA hardware, another possibility is to generate the LO signal from the FPGA and perform phase corrections directly using the FPGA. This can be done by sending a trigger signal to the controller and using it to generate the LO. But this will require two circulators, one for the LO, and the second for beamforming. The feasibility of this technique will have to be explored.

4. Wireless Communication

Wireless data will be passed between the beam controller and the T/R module. The following data types are identified. For the demonstration system, an arbitrary but reasonable 1 Hz control update rate is assumed. At intervals of one second, the beam controller sends waveform parameters, synchronization commands and phase correction commands to each T/R module. The demonstration system will not need to generate

complicated waveforms. Two bits will be sufficient to choose between four possible waveforms, such as continuous sinusoid, pulsed sinusoid and possibly linear frequency modulated waveforms. If wireless distribution of LO is used, two bits are required for synchronization control. One bit is used to send a synchronization command for the T/R module to go into synchronization mode. Another bit is used to send phase correction command for the T/R module to step its phase shifter by $22.5°$.

Transmission of the digitized radar signals takes up a significant portion of the wireless communication. After the phase and amplitude of the received radar signals are recovered, each T/R module sends the 16 bit digitized phase and amplitude data at a rate of 100 kS/s. This works out to a transmission rate of about 3.2 Mb/s for one T/R module.

For the demonstration system, it is assumed that position location is not required. Even if position estimation is needed, TOF and TDOA techniques will operate independently of the wireless link. The beam controller will calculate and translate this information into the required phase weight control information that is sent to the T/R modules. A summary of the wireless data requirements is shown in Table 4.

Description	**From**	**Data rate**
Waveform control	Beam controller	2 bit/s
Synchronization control	Beam controller	1 bit/s for synchronization command 1 bit/s for phase correction command
Phase weights control	Beam controller	4 bit/s
Received radar signals	T/R module	16 bit × 2 ×100 kS/s = 3,200,000 bit/s = 3.2 Mb/s

Table 4. Summary of wireless data requirements.

For a two-element demonstration system, a commercially available wireless access point device can meet the wireless communication requirements. The ASUS WL-330g pocket wireless access point shown in Figure 35 is capable of a maximum transmission rate of 54 Mb/s for orthogonal frequency division multiplexing (OFDM) modulation scheme.

Figure 35. ASUS WL-330Gg pocket wireless access point.

C. WIRELESS COMMUNICATION SOLUTIONS FOR WNODAR

A full-scale implementation of the WNODAR with the projected number of 1200 elements increases the requirements for wireless communication by the same order of magnitude. Based on the data rate of 3.2 Mb/s estimated for a two-element array, the WNODAR will require a data rate of more than 3.7 Gb/s. Therefore implementation of a full-scale WNODAR based on commercial technologies depends on the development of high data rate wireless communication solutions that offer gigabit transmission rates. The following section presents a survey of state-of-the-art and commercially available high data rate wireless systems.

1. Overview of Commercial Wireless Communication Systems

Commercial wireless communication systems are broadly classified as “Wi-Fi” referring to the IEEE 802.11 standard and “WiMAX” referring to the 802.16 standard. “Wi-Fi” is the WLAN standard for relatively short distances, limited to only 30 to 100 m. “WiMAX” on the other hand is designed for outdoor environments and can provide broadband wireless access up to 15 km [30].

“Wi-Fi” was intended to be used for mobile devices and LANs, but is now often used for internet access. “Wi-Fi” technologies have begun to mature and such systems are readily available. They operate in the 2.4 and 5 GHz bands and can have a data rate of up to 54 Mb/s in 20 MHz frequency bands. But the actual throughput is highly dependent on the medium access control (MAC) protocol. Modulation techniques

include orthogonal frequency division multiplexing (OFDM), complimentary code keying (CCK) and packet binary convolutional coding (PBCC). OFDM is a popular method for high data rate wireless transmission. It is a multicarrier modulation scheme where the data is split up among several closely spaced subcarriers. By doing so, OFDM systems are able to provide reliable operation even in environments that result in a high degree of signal distortion due to multipath.

An alternative approach to WLANs is ultrawideband technology (UWB), which has become an area of interest since the FCC recently approved the deployment of UWB on an unlicensed basis in the 3.1 to 10.6 GHz band subject to a revision of the allowed power spectral density. UWB transmits binary data using low-energy and extremely short duration impulses of RF energy. UWB systems are currently designed to achieve transmission rates of 100 Mb/s. Although developers claim that the UWB can hit speeds up to 480 Mb/s, its main drawback is a limited 15 to 100 m transmission range [31]. Another approach using infra red (IR) networking uses radiation with wavelength of 920 to 890 nm can achieve data rates from 10 to 100 Mb/s and above. However, major sources of performance degradation with IR include multipath dispersion, shadowing, and background noise such as sunlight and fluorescent light.

"WiMAX" systems are designed to provide a wireless alternative to cable and DSL for the "last mile" broadband access. The 802.16a standard is designed for systems operating in bands between 2 GHz to 11 GHz. Data rates range from 4.2 to 22.91 Mb/s in a typical bandwidth of 6 MHz. The 802.16d specification eliminates LOS requirements by using OFDM. The 802.16d systems mainly operate in both licensed (2.5 to 2.69 GHz and 3.4 to 3.6 GHz) and unlicensed spectrums (5.725 to 5.850 GHz). A data rate of 37 Mb/s in 10 MHz channel and 11 Mb/s in 3.5 MHz channel has been reported [30].

There are also "WiMAX" systems that operate in the millimeter wave bands, from 24 GHz to frequencies above 60 GHz. A low cost, fixed wireless access (FWA) system in Japan operating at 26 GHz band can connect to a maximum of 239 users, providing transmission capacity of 80 Mb/s in channels with 30 MHz channel separation [32]. IBM recently announced a prototype, small, low-cost 60 GHz receiver and

transmitter chipset that could transfer data at 630 Mb/s, and can improve in a few years to anywhere from 1 Gb/s to 5 Gb/s. Other more complicated millimeter wave radios have the capability to deliver multigigabit communication services up to 10 Gb/s for distance ranging up to 3.5 km [31]. Laser wireless communications called free space optics (FSO) can support data rates ranging from 155 Mb/s to 2.5 Gb/s with distance ranging from 1 to 5 km. However all these communication systems, especially those above 60 GHz and laser, require unobstructed LOS and are limited by the effect of atmospheric factors.

Table 5 gives a brief overview of the commercial wireless communication systems. Spectral efficiency measured in b/s/Hz [33] is commonly used as a performance metric between wireless communication systems. Currently, most commercial wireless communication systems are not yet capable of gigabit transmission rates. Higher data rate transmissions achieved by UWB systems pay the penalty of low bandwidth efficiency and poor transmission distance. On the other hand, millimeter wave radios require strict LOS conditions. Average spectral efficiency is between 2 to 4 b/s/Hz. Above 60 GHz, bandwidth and spectral efficiency are not crucial since it is currently an unregulated band and high bandwidth transmissions are possible.

System or Standard	**Frequency Range**	**Channel Spacing or Bandwidth**	**Data Rate**	**Spectral efficiency**
802.11a	5.15 to 5.825 GHz	20 MHz	54 Mb/s	2.7 b/s/Hz
802.11g	2.4 to 2.4835 GHz			
UWB	3.1 to 10.6 GHz	2 GHz	100 Mb/s	0.05 b/s/Hz
IR systems	820 to 890 nm Wavelength	-	100 Mb/s	-
802.16a	2 to 11 GHz	6 MHz	4.2 to 22.9 Mb/s	0.7 to 3.82 b/s/Hz
802.16d	2.5 to 2.69 GHz 3.4 to 3.6 GHz 5.725 to 5.85 GHz	10 MHz	37 Mb/s	3.1 to 3.7 b/s/Hz
		3.5 MHz	11 Mb/s	
FWA	26 GHz	30 MHz	80 Mb/s	2.6 b/s/Hz
Millimeter wave radios	Above 60 GHz	-	>1 Gb/s	-
Optical systems	1550 nm Wavelength	-	2.5 Gb/s	-

Table 5. Performance of commercial wireless communication systems.

2. Solution to Gigabit Transmission Rate

Transmission rates and spectral efficiency are often limited by transmit power due to radiation hazard considerations and SNR limits in practical receivers. In theory, a gigabit transmission rate for conventional single-input single output (SISO) wireless link is still possible given a large enough bandwidth [28]. A system with a nominal spectral efficiency of 4 b/s/Hz can achieve 1 Gb/s data rate over 250 MHz bandwidth. But 250 MHz bandwidth is difficult to obtain in frequency bands below 6 GHz, where non-LOS networks are feasible. This amount of bandwidth is easier to obtain in the unregulated 60 GHz frequency range. However frequencies higher than 6 GHz are subject to increased shadowing by obstructions in the propagation path. In addition, since transmit power and SNR have regulatory limits and practical limits respectively, a wide bandwidth transmission will mean a reduction in range. Assuming a path propagation loss exponent of 3.0, the range of a 250 MHz bandwidth system compared to a nominal 10 MHz bandwidth system will drop by a factor of three.

In order to overcome these limitations, an active area of research and the most promising solution to gigabit transmission rate is the multi-input multi-output OFDM (MIMO-OFDM) approach. MIMO links with multiple transmit and multiple receive antennas have been shown to achieve performance gains by using multiple transmission and multiple receiving antennas. Figure 36 shows that a 10×10 MIMO system can deliver 1 Gb/s performance with only 20 MHz bandwidth and still support 80% of the reference range of a SISO system. The spectral efficiency achieved is 50 b/s/Hz. When OFDM is combined with MIMO configuration, the diversity gain is increased and system capacity is further enhanced. However, the downside of MIMO-OFDM system is the increased transceiver complexity and this is currently an active area of research.

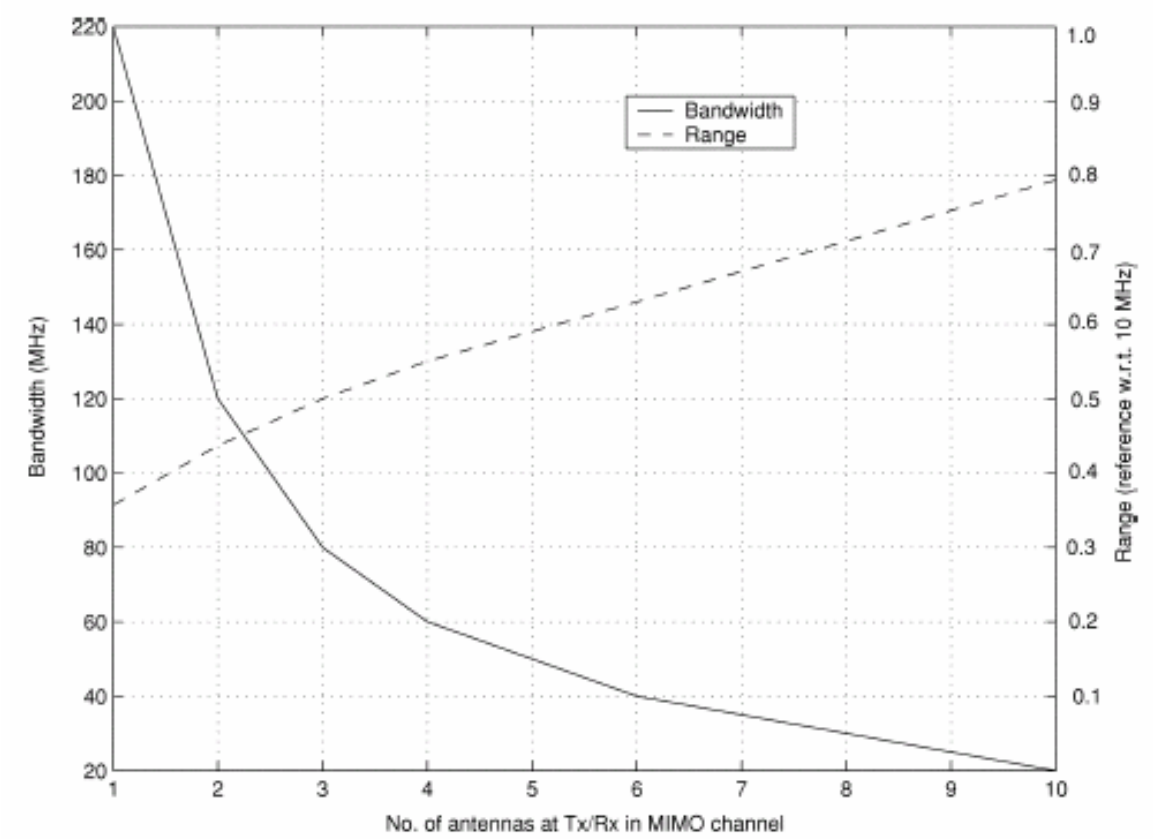

Figure 36. Bandwidth requirement and range of a 1 Gb/s link using MIMO technology (From [28]).

Several efforts to build implementations of MIMO-OFDM have been reported. Iospan demonstrated downlink rates of over 13.6 Mb/s in a 2 MHz channelization over a distance of four miles [34]. This has been equated to over 40 Mbps on a typical 6 MHz channel and a spectral efficiency of 6.7 b/s/Hz. Another prototype reported in [35] demonstrated 1×3 and 2×3 antenna configurations operating between 5.725 to 5.825 GHz using a dual-band bit interleaved coded modulation MIMO-OFDM scheme. It achieved a maximum data rate of 216 Mb/s in a 40 MHz bandwidth. At the same time, to improve on the performance of "WiMAX" systems, enhancements such as spatial multiplexing, spatial diversity coding and space-frequency coded schemes, hybrid automatic repeat request (ARQ), interference cancellation and adaptive subcarrier/power allocation are being studied [36].

Given the current high level of research focus and the unfolding of promising developments towards cheaper, higher performance devices, it appears that the evolution of wireless communication systems to gigabit transmission rates should only be a matter of time. Thus, it is estimated that the requirements of the WNODAR can probably be met with commercial wireless communication systems within the next five years.

D. SUMMARY

This chapter proposed the design of the demonstration T/R module to validate the wireless opportunistic array concept. The design leverages on advance technology adopted from commercial markets, namely the use of FPGA and high data rate wireless communication systems. Based on projected communication requirements, the full-scale WNODAR demands a gigabit transmission rate wireless communication system. Currently, most commercial systems are not yet capable of gigabit transmission rates. But research suggests that MIMO-OFDM technology is a promising solution that could dramatically improve spectral efficiency and thus the viability of gigabit transmission rate. Given the current high level of research focus and the unfolding of promising developments, it is estimated that the requirements of the WNODAR can probably be met with commercial wireless communication systems within the next five years.

THIS PAGE INTENTIONALLY LEFT BLANK

VI. CONCLUSIONS AND RECOMMENDATIONS

A. CONCLUSIONS

The objective of this thesis was to investigate the problem of integrating the array elements of the WNODAR through the design of a wireless synchronization and geolocation network. Phase synchronization of array elements is possible using a simple synchronization circuit. A technical survey of geolocation techniques was performed, and performance curves for the WNODAR operating under different seastate conditions were obtained. Analysis and simulation results suggest that a position location scheme to correct for dynamic effects of hull deflection is not absolutely necessary for an array operating at a VHF or lower UHF frequency. Finally, a design of the demonstration T/R module is proposed. Based on projected communication requirements, the full-scale WNODAR demands a 3.7 Gb/s data transmission rate. The multi-input multi-output orthogonal frequency division multiplexing (MIMO-OFDM) approach has been identified as a promising solution to achieve gigabit transmission rates.

The "brute force" synchronization technique is a simple method that can be easily implemented with a synchronization circuit in each element and in the central beamformer and controller. The "beam tagging" synchronization technique takes less time, but requires more hardware modifications. Since the synchronization time is on the order of 2 to 3 μs, the more simple "brute force" technique is sufficient. It was also concluded that a four-bit synchronization phase shifter does not affect the performance of the radar. The phase error is expected to introduce a gain reduction of 0.06 dB which can be overcome by a 2.8% increase in average transmit power. The expected RMS pointing error of less than $0.001°$ and a mean sidelobe increase of $0.1\,\text{dB}$ with respect to the main lobe is insignificant compared to the error free pattern.

The problem of position determination for elements in a WNODAR can be tackled through commercial solutions for geolocation. Under relatively benign propagation conditions, most systems are producing centimeter level accuracy, which is a fraction of the array's operating wavelength of about 1 m and within the tolerable limit of 0.1λ position error. Using conventional hull deflection data and extrapolating to the

DD(X), a set of performance curves for the WNODAR was obtained. The curves show the performance of the WNODAR operating under dynamic conditions, taking into account the effects of hull deflection under different seastate conditions, and the use of four-bit synchronization phase shifters. For a nominal average transmission power of 500 W, a maximum detection range of 1990 km for a 10 m^2 target is obtained under seastate 6 conditions. This is only a reduction of 0.5% from the error free condition. Hence at this time, analysis and simulation results suggest that a position location scheme to correct for dynamic effects of hull deflection is not absolutely necessary for an array operating at a VHF or lower UHF frequency.

The design of the demonstration T/R module is proposed to validate the wireless opportunistic array concept. The design leverages on advance technology adopted from commercial markets, namely the use of FPGA and high data rate wireless communication systems. Based on projected requirements, the full-scale WNODAR demands a gigabit data transmission rate. Currently, most commercial systems are not yet capable of gigabit transmission rates. But research suggests that MIMO-OFDM technology is a promising solution that could dramatically improve spectral efficiency and thus the viability of gigabit transmission rate. Given the current high level of research focus and the unfolding of promising developments towards cheaper, higher performance devices, it is estimated that the requirements of the WNODAR can probably be met with commercial wireless communication systems within the next five years.

B. RECOMMENDATIONS FOR FUTURE WORK

1. Ship Hull Deflection Data

Ships underway experience whole ship changes in position, orientation, flexures and twists in which the components of the ship move relative to each other. Effort should be made to measure such motions while a ship is underway in various sea states and orientations relative to the waves. The data will be useful for performing more advanced radar system tradeoff studies, as well as for other precision antennas (e.g., ESM equipment or communications).

2. Radar Signal Processing Study

Developmental work is required to write the signal processing and beamforming software for the WNODAR. Techniques, such as real-time beamforming, adaptive nulling, signal filtering, pulse compression and pulse integration, should be studied to improve the radar performance. In particular, issues such as the limits of performance, signal processing bandwidth requirements and additional hardware requirements need to be studied.

3. Hardware Demonstration

A demonstration of a low power T/R module is to be build on National Instruments (NI) compact realtime I/O (CompactRIO) modules. The hardware should be fully tested and its full capability should be exploited. This includes the possibility of eliminating the need for a DDS as well as direct generation and synchronization of LO and waveforms in T/R modules. Also, the time-varying phase shift approach to scanning the transmit beam needs to be demonstrated [9].

4. Wireless Communication

Wireless communication should be demonstrated using CompactRIO modules. At the same time, there is a need to conduct analysis and simulations for the full scale array. Issues such as modulation scheme, error correction coding, antenna design and fading effects in a ship multipath environment, are some areas that need to be addressed.

THIS PAGE INTENTIONALLY LEFT BLANK

LIST OF REFERENCES

[1] Perry, W. J., "1996 Annual Defense Report," United States Department of Defense, 1996.

[2] Williams, J. D., "The Future of AEGIS Ballistic Missile Defense," George C. Marshall Institute, October 2004

[3] Global Security.org, "AN/FPS-108 COBRA DANE," http://www.globalsecurity.org/space/systems/cobra_dane.htm, Retrieved February 2006.

[4] Jenn, D. C., "Aperstructures, opportunistic arrays, and digital beamforming," Presented at the Georgia Tech. Aperstructures Workshop, April 2005.

[5] Primezone Newswire & Multimedia Distribution, "Photo Release - DD(X) national team completes radar cross-section testing of DD(X) deckhouse," http://www.primezone.com/newsroom/news.html?d=83942, Retrieved February 2006.

[6] Jenn, D. C., Program review, "Aperstructures, opportunistic arrays and BMD," Naval Postgraduate School, October 2005 (unpublished).

[7] Esswein, L. C., "Genetic algorithm design and testing of a random element 3-D 2.4 GHz phased array transmit antenna constructed of commercial RF microchips," Master's Thesis, Naval Postgraduate School, Monterey, California, June 2003.

[8] Eng, C. S., "Digital antenna architectures using commercial off the shelf hardware," Master's Thesis, Naval Postgraduate School, Monterey, California, December 2003.

[9] Ong, C. S., "Digital phased array architectures for radar and communications based on off-the-shelf wireless technologies," Master's Thesis, Naval Postgraduate School, Monterey, California, December 2004.

[10] Tong, C. H., "System study and design of broad-band U-slot microstrip patch antennas for aperstuctures and opportunistic arrays," Master's Thesis, Naval Postgraduate School, Monterey, California, December 2005.

[11] Yong, Y. C., "Receive channel architecture and transmission system for digital array radar," Master's Thesis, Naval Postgraduate School, Monterey, California, December 2005.

[12] Ong, W., "Commercial off the shelf direct digital synthesizers for digital array radar," Master's Thesis, Naval Postgraduate School, Monterey, California, December 2005.

[13] Jenn, D. C., Program review, "Wirelessly networked opportunistic digital array radar," Naval Postgraduate School, January 2006 (unpublished).

[14] Skolnik, M. I., *Introduction to Radar Systems*, 3rd edition, McGraw-Hill, New York, pp. 636, 2001.

[15] Adams, R. T., "Beam tagging for control of adaptive transmitting arrays," *IEEE Transactions on Antennas and Propagation*, Vol. AP-12, pp. 224-227, March 1964.

[16] East, T. W. R., "A self-steering array for the SHARP microwave-powered aircraft," *IEEE Transactions on Antennas and Propagation*, Vol. 30, No. 12, pp. 1565, December 1992.

[17] Steinberg, B. D., *Principles of Aperture and Array System Design*, John Wiley & Sons, Inc., pp. 308-316, 1975.

[18] Taheri, S. H. and Steinberg, B. D., "Tolerance in self-cohering antenna arrays of arbitrary geometry," *IEEE Transactions on Antennas and Propagation*, Vol. AP-24, No. 5, pp. 733-739, September 1976.

[19] Garmin International Inc., "What is GPS?," http://www.garmin.com/aboutGPS/, Retrieved February 2006.

[20] Boseley, K. and Waid, J., "Demonstration system for using shipboard-relative GPS," *GPS World*, pp. 24-33, April 2005.

[21] Barnes, J., Rizos, C., Wang, J., Small, D., Voigt, G. and Gambale, N., "Locata: the positioning technology of the future?," Presented at SatNav 2003, The 6th International Symposium on Satellite Navigation Technology Including Mobile Positioning & Location Services, Melbourne, Australia, July 2003.

[22] Bahl, P. and Padmanabhan, V., "RADAR: An in-building RF-based user location and tracking system," *Proc. IEEE Infocom 2000*, IEEE CS Press, Los Alamitos, pp. 775-784, Calif., 2000.

[23] M.I.T. Computer Science and Artificial Intelligence Laboratory, "The Cricket indoor location system," http://nms.lcs.mit.edu/projects/cricket/#overview, Retrieved February 2006.

[24] ELVA-1 Millimeter Wave Division, "FMCW 94/10 millimeter wave distance sensor," http://www.elva-1.spb.ru, Retrieved January 2006

[25] Fontana, R. J. and Gunderson, S. J., "Ultra-wideband precision asset location System," *IEEE Conference on Ultra Wideband Systems and Technologies*, pp. 147-150, 2002.

[26] Mennitt, S. H., "The effects of ship load variations and seastate on hull girder deflection and combat system alignment," Master's Thesis, Massachusetts Institute of Technology, September 1990.

[27] Interactive Circuits and Systems, "The rising importance of FPGA technology in software defined radio," http://www.cotsjournalonline.com, December 2005.

[28] Paulraj, A. J., "An overview of MIMO communications – A key to gigabit Wireless," *Proceedings of the IEEE*, Vol. 92, No. 2, pp. 198-218, February 2004.

[29] National Instruments, "NI CompactRIO – Reconfigurable control and acquisition system," http://www.ni.com/compactrio/whatis.htm, Retrieved February 2006.

[30] Conti, J. P., "The long road to WiMAX," *IEE Review*, pp. 39-42, October 2005.

[31] Zeadally, S. and Zhang, L., "Enabling gigabit network access to end users," *Proceedings of the IEEE*, Vol. 92, No. 2, pp. 340-353, February 2004.

[32] Kimura, Y., Miura, Y., Shirosaki, T., Taniguchi, T., Kazama, Y., Hirokawa, J., Ando, M., and Shirouzu, T., "A Low Cost and Very Compact Wireless Terminal Integrated on the Back of a Waveguide Planar Array for 26 GHz Band Fixed Wireless Access (FWA) Systems," *IEEE Transactions on Antennas and Propagation*, Vol. 53, No. 8, pp.2456-2463, August 2005.

[33] Roy, S., Foerster, J. R., Somayazulu, V. S. and Leeper, D. G., "Ultrawideband radio design: The promise of high-speed, short-range wireless connectivity," *Proceedings of the IEEE*, Vol. 92, No. 2, pp. 297, February 2004.

[34] Mason, C. F., "First days of 2002 offer good news," *Broadband Wireless Online*, February 2002.

[35] Yu, H., Kim, M. S., Choi, E., Jeon, T. and Lee, S., "Design and prototype development of MIMO-OFDM for next generation wireless LAN," *IEEE Transactions on Consumer Electronics*, Vol. 51, No. 4, pp. 1134-1142, November 2005.

[36] Ghosh, A. and Wolter, D. R., "Broadband wireless access with WiMAX/802.1: Current Performance Benchmarks and Future Potential," *IEEE Communications Magazine*, pp. 129-136, February 2005.

THIS PAGE INTENTIONALLY LEFT BLANK

INITIAL DISTRIBUTION LIST

1. Defense Technical Information Center
   Ft. Belvoir, Virginia

2. Dudley Knox Library
   Naval Postgraduate School
   Monterey, California

3. Professor David C. Jenn
   Department of Electrical & Computer Engineering
   Naval Postgraduate School
   Monterey, California

4. Chairman, Code EC
   Department of Electrical and Computer Engineering
   Naval Postgraduate School
   Monterey, California

5. James King
   Office of Naval Research
   Arlington, Virginia

6. Professor Michael A. Morgan
   Department of Electrical & Computer Engineering
   Naval Postgraduate School
   Monterey, California

7. Professor Michael Melich
   Wayne E. Meyer Institute of System Engineering
   Naval Postgraduate School
   Monterey, California

8. Professor Rodney Johnson
   Wayne E. Meyer Institute of System Engineering
   Naval Postgraduate School
   Monterey, California

9. Professor Bill Solitario
   Wayne E. Meyer Institute of System Engineering
   Naval Postgraduate School
   Monterey, California

10. Yeo Siew Yam
DSO National Labs
Singapore

11. LCDR Gert Burgstaller, Code: EC596
Naval Postgraduate School
Monterey, California

12. MAJ Loke Yong
Ministry of Defence
Singapore